A theoretical survey of atomic structure and forbidden transitions in the $4p^k$ and $4d^k$ ground configurations of tungsten ions W^{29+} through W^{43+}

2012 J. Phys. B: At. Mol. Opt. Phys. 45 025003

(http://iopscience.iop.org/0953-4075/45/2/025003)

J. Phys. B: At. Mol. Opt. Phys. **45** (2012) 025003 (15pp) doi:10.1088/0953-4075/45/2/025003

A theoretical survey of atomic structure and forbidden transitions in the $4p^k$ and $4d^k$ ground configurations of tungsten ions W^{29+} through W^{43+}

Pascal Quinet

Astrophysique et Spectroscopie, Université de Mons—UMONS, B-7000 Mons, Belgium
and
IPNAS, Université de Liège, B15 Sart Tilman, B-4000 Liège, Belgium

E-mail: quinet@umons.ac.be

Received 19 September 2011, in final form 25 November 2011
Published 22 December 2011
Online at stacks.iop.org/JPhysB/45/025003

Abstract
Energy levels, wavelengths and radiative decay rates have been calculated for states within the $4p^k$ ($k = 1$–5) and $4d^k$ ($k = 1$–9) ground configurations in highly charged tungsten ions. Magnetic dipole (M1) and electric quadrupole (E2) transition probabilities have been obtained using the fully relativistic multiconfiguration Dirac–Fock (MCDF) approach including the correlations within the $n = 4$ complex, some $n = 4 \rightarrow n' = 5$ single excitations and quantum electrodynamics effects. The validity of the method is assessed through limited comparison with experimental and theoretical data previously published as well as with new relativistic Hartree–Fock calculations. The excellent agreement observed between our new MCDF *A*-values and those obtained using different theoretical approaches together with a detailed analysis of configuration interaction effects does not confirm the very recent GRASP2K calculations of Jonauskas *et al* (2012 *At. Data Nucl. Data Tables* **98** 19) for M1 lines within the $4d^k$ configurations, the latter results remaining in large disagreement with all other methods in many cases.

1. Introduction

Atomic data of tungsten are strongly needed for the identification and interpretation of emission lines from future fusion reactors (such as ITER), which will use this element as plasma-facing material (see e.g. Matthews *et al* 2007, Pitts *et al* 2009, Hawryluk *et al* 2009). In this context, forbidden lines are of great interest for plasma diagnostics because the corresponding radiation intensities are often very sensitive to electron temperature and density. Consequently, reliable radiative data for such forbidden lines in different ionization stages of tungsten are to be determined from experimental measurements or theoretical calculations.

On the experimental side, several studies led to the identification of a bit more than a hundred of the forbidden lines in tungsten ions, from W^{28+} to W^{57+} in a tokamak or electron-beam ion trap (EBIT) from ultraviolet to x-ray regions (Tragin *et al* 1988, Neu *et al* 1997, 2001, Porto *et al* 2000, Utter *et al* 2000, Pütterich *et al* 2005, Radtke *et al* 2007, Ralchenko *et al* 2006, 2007, 2008, 2011a, Clementson *et al* 2010). All of these data were compiled at the National Institute of Standards and Technology (NIST) by Ralchenko *et al* (2011b) who critically evaluated wavelengths for observed lines and energy levels for many ionization stages of tungsten. Together with the previously published analyses of the spectra of neutral and singly ionized tungsten by Kramida and Shirai (2006) and of multiply charged ions W^{2+} through W^{73+} by Kramida and Shirai (2009), NIST compilation provides reference data for all tungsten spectra including magnetic dipole and electric quadrupole radiation.

Forbidden transitions in tungsten ions were also investigated using different theoretical methods over the last few decades. More precisely, the multiconfiguration Dirac–Fock method was used for computing transition probabilities for forbidden lines in the $3p^k$ configurations in W^{57+} (Huang *et al* 1983), W^{58+} (Saloman and Kim 1989), W^{59+} (Huang

1984), W^{60+} (Huang 1985) and W^{61+} (Huang 1986). Feldman *et al* (1991, 2001) and Doron and Feldman (2001) performed a systematic study of density-sensitive magnetic dipole lines in Ti-like ions including W^{53+}. Fully relativistic, *ab initio* calculations of wavelengths and oscillator strengths were carried out by Fournier (1998) for 11 tungsten ions from Rb-like W^{37+} to Co-like W^{47+}. Decay rates for forbidden lines were also obtained by Charro *et al* (2002, 2003) for W^{55+} and W^{61+} ions using the relativistic quantum defect orbital (RQDO) approach, by Safronova and Safronova (2010) for W^{4+}, W^{27+}, W^{44+}, W^{54+}, W^{61+}, W^{62+}, W^{69+} and W^{70+} ions using the relativistic many-body perturbation theory (RMBPT) and by Quinet *et al* (2010) for W, W^{+} and W^{2+} species using the relativistic Hartree–Fock (HFR) method. Using the relativistic flexible atomic code (FAC), Ralchenko *et al* (2011a) calculated wavelengths and transition probabilities corresponding to some forbidden lines within the $3d^k$ (k = 1–9) ground configurations of tungsten ions W^{47+} through W^{55+}. This work was considerably extended in our recent work (Quinet 2011) in which forbidden transitions connecting all energy levels within the $3p^k$ (k = 1–5) and $3d^k$ (k = 1–9) configurations in tungsten ions from W^{47+} to W^{61+} were investigated using the multiconfiguration Dirac–Fock (MCDF) method. Magnetic dipole transitions between levels of the $4d^k$ ground configurations of tungsten ions W^{29+} through W^{37+} were analysed using large-scale configuration interaction methods by Jonauskas *et al* (2010) who reported theoretical wavelengths and transition probabilities for a limited number (45) of lines between 44 and 98 nm. Finally, very recently, relativistic calculations for M1 transitions in the $4d^k$ configurations of W^{29+}–W^{37+} ions using the GRASP2K code were carried out by Jonauskas *et al* (2012) who observed large discrepancies with theoretical transition probabilities previously published.

The aim of this paper is to extend these works by investigating the magnetic dipole and electric quadrupole transitions involving all of the levels belonging to the ground configurations of highly charged tungsten ions with an open 4d shell (W^{29+}–W^{37+}) or an open 4p shell (W^{39+}–W^{43+}). For these lines, energy levels, wavelengths and transition probabilities were computed using the fully relativistic MCDF method including the most important configuration interaction effects as well as quantum electrodynamics (QED) corrections. The theoretical model used as well as a comparison between all available data is presented in detail in the following sections.

2. Theoretical approach

The investigation of highly charged tungsten ions considered in this paper requires the simultaneous consideration of electronic correlation and relativistic effects. The MCDF method in the form developed by Grant and coworkers (Grant *et al* 1980, McKenzie *et al* 1980) is ideal for this purpose. Consequently, this approach was used in this paper with the latest version of GRASP, the general-purpose relativistic atomic structure package, developed by Norrington (2009). The computations were performed in the extended average level (EAL) mode in which a weighted trace of the Hamiltonian is optimized using level weights proportional to $2J+1$. This was completed with the inclusion of the relativistic two-body Breit interaction and the QED corrections due to self-energy and vacuum polarization using the routines developed by McKenzie *et al* (1980). In these routines, the leading corrections to the Coulomb repulsion between electrons in QED are considered as a first perturbation using the transverse Breit operator given by Grant and McKenzie (1980), the second-order vacuum polarization corrections are evaluated using the prescription of Fullerton and Rinker (1976) and the self-energy contributions are estimated by interpolating the hydrogenic $n = 1, 2$ results of Mohr (1974, 1975) and by scaling to higher n states according to $1/n^3$. Moreover, the nuclear effects were estimated by considering a uniform charge distribution with the usual atomic weight of tungsten, i.e. 183.85.

For the $4p^k$ configurations (ions W^{39+}–W^{43+}), single and double excitations within the $n = 4$ complex together with single excitations from 4p to 5p and 5f orbitals were considered by including the configurations of the type $4s^24p^k + 4p^{k+2} + 4s4p^k4d + 4s^24p^{k-2}4d^2 + 4s^24p^{k-2}4f^2 + 4p^k4d^2 + 4p^k4f^2 + 4s^24p^{k-1}4f + 4s^24p^{k-1}5p + 4s^24p^{k-1}5f$. In a similar way, for the $4d^k$ configurations (ions W^{29+}–W^{37+}), single and double excitations within the $n = 4$ complex together with single excitations from 4d to 5s and 5d orbitals were included by considering the following multiconfiguration expansions: $4s^24p^64d^k + 4s^24p^44d^{k+2} + 4s4p^64d^{k+1} + 4p^64d^{k+2} + 4s^24p^54d^k4f + 4s^24p^64d^{k-2}4f^2 + 4s^24p^64d^{k-1}5s + 4s^24p^64d^{k-1}5d$. A detailed list of electronic configurations included in the calculations for each tungsten ion is given in table 1. It is interesting to note that most of the configurations included in the latter model have the strongest interaction with $4d^k$, as demonstrated by Jonauskas *et al* (2010) who calculated the configuration interaction strengths between the $4d^k$ configuration and about 50 other configurations. It was also shown by the latter authors that the most important mixings for those configurations are determined near the half-filled 4d shell, where the number of configuration state functions is the largest.

When performing our calculations, we noted that the most important configuration interactions affecting the $4s^24p^k$ configurations were due to $4p^{k+2}$, $4s4p^k4d$ and $4s^24p^{k-2}4d^2$, while, for the $4s^24d^k$ configurations, the largest mixings involved $4s^24p^54d^k4f$, $4s^24p^44d^{k+2}$ and $4s^24p^64d^{k-2}4f^2$.

For the energy levels of interest, i.e. those belonging to the $4p^k$ and $4d^k$ configurations, the relativistic two-body Breit corrections were found to vary from 330 to 16700 cm^{-1}, while QED effects were found to vary from 0 to 1700 cm^{-1}. This represents relative contributions to the total energies ranging from 0.5% to 2.7 % for Breit interaction and from 0% to 0.12% for QED effects.

3. Energy level structure

Energy levels calculated in this work using the MCDF method described above for the $4p^k$ and $4d^k$ ground configurations in tungsten ions from W^{29+} to W^{43+} are reported in table 2. For each level, the main component of the computed eigenvector

Table 1. Electronic configurations included in MCDF calculations of forbidden transitions within the $4p^k$ and $4d^k$ ground configurations of tungsten ions.

Ion	Configurations
W^{29+}	$4s^24p^64d^9 + 4s4p^64d^{10} + 4s^24p^54d^94f + 4s^24p^64d^74f^2 + 4s^24p^64d^85s + 4s^24p^64d^85d$
W^{30+}	$4s^24p^64d^8 + 4s^24p^44d^{10} + 4s4p^64d^9 + 4p^64d^{10} + 4s^24p^54d^84f + 4s^24p^64d^64f^2 + 4s^24p^64d^75s + 4s^24p^64d^75d$
W^{31+}	$4s^24p^64d^7 + 4s^24p^44d^9 + 4s4p^64d^8 + 4p^64d^9 + 4s^24p^54d^74f + 4s^24p^64d^54f^2 + 4s^24p^64d^65s + 4s^24p^64d^65d$
W^{32+}	$4s^24p^64d^6 + 4s^24p^44d^8 + 4s4p^64d^7 + 4p^64d^8 + 4s^24p^54d^64f + 4s^24p^64d^44f^2 + 4s^24p^64d^55s + 4s^24p^64d^55d$
W^{33+}	$4s^24p^64d^5 + 4s^24p^44d^7 + 4s4p^64d^6 + 4p^64d^7 + 4s^24p^54d^54f + 4s^24p^64d^34f^2 + 4s^24p^64d^45s + 4s^24p^64d^45d$
W^{34+}	$4s^24p^64d^4 + 4s^24p^44d^6 + 4s4p^64d^5 + 4p^64d^6 + 4s^24p^54d^44f + 4s^24p^64d^24f^2 + 4s^24p^64d^35s + 4s^24p^64d^35d$
W^{35+}	$4s^24p^64d^3 + 4s^24p^44d^5 + 4s4p^64d^4 + 4p^64d^5 + 4s^24p^54d^34f + 4s^24p^64d4f^2 + 4s^24p^64d^25s + 4s^24p^64d^25d$
W^{36+}	$4s^24p^64d^2 + 4s^24p^44d^4 + 4s4p^64d^3 + 4p^64d^4 + 4s^24p^54d^24f + 4s^24p^64f^2 + 4s^24p^64d5s + 4s^24p^64d5d$
W^{37+}	$4s^24p^64d + 4s^24p^44d^3 + 4s4p^64d^2 + 4p^64d^3 + 4s^24p^54d4f + 4s^24p^65s + 4s^24p^65d$
W^{39+}	$4s^24p^5 + 4s4p^54d + 4s^24p^34d^2 + 4s^24p^34f^2 + 4p^54d^2 + 4p^54f^2 + 4s^24p^44f + 4s^24p^45p + 4s^24p^45f$
W^{40+}	$4s^24p^4 + 4p^6 + 4s4p^44d + 4s^24p^24d^2 + 4s^24p^24f^2 + 4p^44d^2 + 4p^44f^2 + 4s^24p^34f + 4s^24p^35p + 4s^24p^35f$
W^{41+}	$4s^24p^3 + 4p^5 + 4s4p^34d + 4s^24p4d^2 + 4s^24p4f^2 + 4p^34d^2 + 4p^34f^2 + 4s^24p^24f + 4s^24p^25p + 4s^24p^25f$
W^{42+}	$4s^24p^2 + 4p^4 + 4s4p^24d + 4s^24d^2 + 4s^24f^2 + 4p^24d^2 + 4p^24f^2 + 4s^24p4f + 4s^24p5p + 4s^24p5f$
W^{43+}	$4s^24p + 4p^3 + 4s4p4d + 4p4d^2 + 4p4f^2 + 4s^24f + 4s^25p + 4s^25f$

in both *LS*- and *jj*-coupling schemes is also given in that table. In the *jj* notation adopted, nl_- corresponds to the case $j_- = l - 1/2$, while nl is written for $j_+ = l + 1/2$. As seen from the table and as expected for such highly ionized atoms, *jj* coupling appears much more adequate than the *LS* one, the average *jj* purities obtained in this work being found to be equal to 99% and 84%, for the $4p^k$ and $4d^k$ configurations, respectively, while the corresponding average *LS* contributions are found to range from 77% to 52%. Consequently, the *jj* designation has been used throughout this paper. For simplicity, in table 2 each energy level belonging to a particular ion is labelled as $nl^k[i]_J$, where nl^k is the electronic configuration, i is an order number in this configuration and J is the total angular momentum.

Our results are also compared in table 2 with available energy levels taken from the latest NIST compilation (Ralchenko *et al* 2011b), which is entirely based on the data listed by Kramida and Shirai (2009) for the ions considered in the present paper. For the $4p^k$ and $4d^k$ configurations, the experimental energy levels reported in these compilations were originally determined from emission spectra observed by Radtke *et al* (2007) for W^{29+} through W^{37+} ions, by Ralchenko *et al* (2007) for W^{39+} and W^{42+} ions, by Pütterich *et al* (2005) for W^{40+}, W^{41+} and W^{43+} ions and by Utter *et al* (2002) for W^{40+}. All of the other NIST values were calculated by Kramida and Shirai (2009) using parametric fitting with Cowan's codes (Cowan 1981). When comparing our MCDF results with experimental energies, good agreement is observed, the average relative differences being found to be equal to 0.2% (W^{29+}), 1.1% (W^{30+}), 0.5% (W^{31+}), 0.1% (W^{32+}), 0.8% (W^{33+}), 0.7% (W^{34+}), 1.0% (W^{35+}), 1.4% (W^{36+}), 0.3% (W^{37+}), 0.7% (W^{39+}), 0.6% (W^{40+}), 0.3% (W^{41+}), 0.2% (W^{42+}) and 0.1% (W^{43+}). However, larger discrepancies (up to 20%) can be observed between our energy levels with those calculated by Kramida and Shirai (2009) but it may reasonably be expected that, for highly ionization degrees such as those considered here, the fully relativistic MCDF method used in our work should be more appropriate than the Hartree–Fock approximation used by Kramida and Shirai (2009) where relativistic effects were included perturbationally.

4. Wavelengths and transition probabilities for forbidden lines

Wavelengths and transition probabilities for magnetic dipole (M1) and electric quadrupole (E2) transitions within the $4p^k$ and $4d^k$ ground configurations of tungsten ions were computed using the MCDF method described above. Results are listed in table 3 for lines with A-values greater than 10^4 s^{-1} except a few weaker lines observed experimentally. If the two types of radiations contribute significantly to the total intensity of a line, the sum of both A-values is given in the table. The exclusion criterion of one particular type of radiation for a given transition is that the corresponding transition probability should be less than 1% of the sum of M1 and E2 contributions. As already noted in our previous work on the $3p^k$ and $3d^k$ configurations (Quinet 2011), M1 contributions were found to dominate by far E2 ones in the $4d^k$ configurations, while both

Table 2. Energy levels within the $4p^k$ and $4d^k$ ground configurations of tungsten ions.

Ion	Label	*LS* purity	*jj* purity	E_{MCDF}[a] (10^3 cm^{-1})	E_{NIST}[b] (10^3 cm^{-1})
W^{29+}	$4d^9[1]_{5/2}$	98% $^2D_{5/2}$	98% $((4d^4_-)_0(4d^5)_{5/2})_{5/2}$	0.00	0.0
	$4d^9[2]_{3/2}$	98% $^2D_{3/2}$	98% $((4d^3_-)_{3/2}(4d^6)_0)_{3/2}$	132.44	132.16
W^{30+}	$4d^8[1]_4$	88% $^3F_4$	97% $((4d^4_-)_0(4d^4)_4)_4$	0.00	0.0
	$4d^8[2]_2$	49% $^1D_2$	98% $((4d^4_-)_0(4d^4)_2)_2$	26.60	[25.3]
	$4d^8[3]_0$	57% $^3P_0$	95% $((4d^4_-)_0(4d^4)_0)_0$	83.09	[83.0]
	$4d^8[4]_3$	98% $^3F_3$	98% $((4d^3_-)_{3/2}(4d^5)_{5/2})_3$	126.70	125.91
	$4d^8[5]_2$	51% $^3P_2$	96% $((4d^3_-)_{3/2}(4d^5)_{5/2})_2$	154.34	151.83?
	$4d^8[6]_1$	98% $^3P_1$	98% $((4d^3_-)_{3/2}(4d^5)_{5/2})_1$	168.11	170.74
	$4d^8[7]_4$	88% $^1G_4$	97% $((4d^3_-)_{3/2}(4d^5)_{5/2})_4$	175.22	175.31
	$4d^8[8]_2$	54% $^3F_2$	97% $((4d^2_-)_2(4d^6)_0)_2$	275.80	279.54?
	$4d^8[9]_0$	57% $^1S_0$	95% $((4d^2_-)_0(4d^6)_0)_0$	352.11	[355.0]
W^{31+}	$4d^7[1]_{9/2}$	63% $^4F_{9/2}$	96% $((4d^4_-)_0(4d^3)_{9/2})_{9/2}$	0.00	0.0
	$4d^7[2]_{3/2}$	49% $^2P_{3/2}$	97% $((4d^4_-)_0(4d^3)_{3/2})_{3/2}$	36.35	
	$4d^7[3]_{5/2}$	35% $^2D_{5/2}$	92% $((4d^4_-)_0(4d^3)_{5/2})_{5/2}$	55.88	
	$4d^7[4]_{7/2}$	86% $^4F_{7/2}$	78% $((4d^3_-)_{3/2}(4d^4)_4)_{7/2}$	124.91	124.24
	$4d^7[5]_{9/2}$	34% $^2H_{9/2}$	95% $((4d^3_-)_{3/2}(4d^4)_4)_{9/2}$	150.66	149.98
	$4d^7[6]_{3/2}$	35% $^4F_{3/2}$	83% $((4d^3_-)_{3/2}(4d^4)_2)_{3/2}$	153.66	
	$4d^7[7]_{5/2}$	59% $^4P_{5/2}$	93% $((4d^3_-)_{3/2}(4d^4)_4)_{5/2}$	159.02	
	$4d^7[8]_{1/2}$	51% $^4P_{1/2}$	98% $((4d^3_-)_{3/2}(4d^4)_2)_{1/2}$	165.37	
	$4d^7[9]_{11/2}$	98% $^2H_{11/2}$	98% $((4d^3_-)_{3/2}(4d^4)_4)_{11/2}$	177.45	
	$4d^7[10]_{7/2}$	50% $^2G_{7/2}$	67% $((4d^3_-)_{3/2}(4d^4)_2)_{7/2}$	192.86	
	$4d^7[11]_{5/2}$	66% $^2F_{5/2}$	92% $((4d^3_-)_{3/2}(4d^4)_2)_{5/2}$	209.48	
	$4d^7[12]_{3/2}$	43% $^2D_{3/2}$	73% $((4d^3_-)_{3/2}(4d^4)_0)_{3/2}$	259.58	
	$4d^7[13]_{5/2}$	55% $^4F_{5/2}$	83% $((4d^2_-)_2(4d^5)_{5/2})_{5/2}$	276.49	
	$4d^7[14]_{3/2}$	36% $^4P_{3/2}$	90% $((4d^2_-)_2(4d^5)_{5/2})_{3/2}$	287.07	
	$4d^7[15]_{1/2}$	51% $^2P_{1/2}$	98% $((4d^2_-)_2(4d^5)_{5/2})_{1/2}$	302.79	
	$4d^7[16]_{9/2}$	60% $^2H_{9/2}$	98% $((4d^2_-)_2(4d^5)_{5/2})_{9/2}$	306.04	
	$4d^7[17]_{7/2}$	52% $^2F_{7/2}$	92% $((4d^2_-)_2(4d^5)_{5/2})_{7/2}$	316.68	
	$4d^7[18]_{5/2}$	53% $^2D_{5/2}$	84% $((4d^2_-)_0(4d^5)_{5/2})_{5/2}$	388.92	
	$4d^7[19]_{3/2}$	39% $^2D_{3/2}$	95% $((4d_-)_{3/2}(4d^6)_0)_{3/2}$	445.83	
W^{32+}	$4d^6[1]_4$	38% $^5D_4$	93% $((4d^4_-)_0(4d^2)_4)_4$	0.00	0.0
	$4d^6[2]_2$	22% $^3P_2$	93% $((4d^4_-)_0(4d^2)_2)_2$	21.75	[21.4]
	$4d^6[3]_0$	47% $^3P_0$	82% $((4d^4_-)_0(4d^2)_0)_0$	70.11	[56.0]
	$4d^6[4]_3$	68% $^5D_3$	77% $((4d^3_-)_{3/2}(4d^3)_{9/2})_3$	113.87	[122.0]
	$4d^6[5]_4$	40% $^5D_4$	84% $((4d^3_-)_{3/2}(4d^3)_{9/2})_4$	124.59	124.53
	$4d^6[6]_1$	53% $^5D_1$	56% $((4d^3_-)_{3/2}(4d^3)_{3/2})_1$	127.94	[134.0]
	$4d^6[7]_5$	59% $^3G_5$	98% $((4d^3_-)_{3/2}(4d^3)_{9/2})_5$	151.07	151.27
	$4d^6[8]_6$	68% $^3H_6$	97% $((4d^3_-)_{3/2}(4d^3)_{9/2})_6$	153.24	[153.0]
	$4d^6[9]_2$	48% $^3F_2$	75% $((4d^3_-)_{3/2}(4d^3)_{3/2})_2$	167.67	[163.0]
	$4d^6[10]_3$	28% $^3G_3$	62% $((4d^3_-)_{3/2}(4d^3)_{3/2})_3$	172.84	[170.0]
	$4d^6[11]_0$	67% $^3P_0$	67% $((4d^3_-)_{3/2}(4d^3)_{3/2})_0$	203.01	[194.0]
	$4d^6[12]_2$	36% $^3D_2$	62% $((4d^3_-)_{3/2}(4d^3)_{5/2})_2$	209.71	[197.0]
	$4d^6[13]_1$	37% $^3D_1$	51% $((4d^3_-)_{3/2}(4d^3)_{5/2})_1$	210.90	[201.0]
	$4d^6[14]_4$	37% $^1G_4$	84% $((4d^3_-)_{3/2}(4d^3)_{5/2})_4$	213.40	[199.0]
	$4d^6[15]_3$	41% $^3F_3$	67% $((4d^3_-)_{3/2}(4d^3)_{5/2})_3$	222.81	[211.0]
	$4d^6[16]_2$	53% $^5D_2$	79% $((4d^2_-)_2(4d^4)_4)_2$	251.33	[258.0]
	$4d^6[17]_0$	57% $^5D_0$	77% $((4d^2_-)_2(4d^4)_2)_0$	262.33	[263.0]
	$4d^6[18]_4$	41% $^3H_4$	67% $((4d^2_-)_2(4d^4)_4)_4$	274.10	[277.0]
	$4d^6[19]_3$	28% $^3D_3$	83% $((4d^2_-)_2(4d^4)_4)_3$	284.26	[285.0]
	$4d^6[20]_5$	59% $^3H_5$	98% $((4d^2_-)_2(4d^4)_4)_5$	288.21	[290.0]
	$4d^6[21]_6$	68% $^1I_6$	97% $((4d^2_-)_2(4d^4)_4)_6$	302.57	302.658
	$4d^6[22]_3$	44% $^3G_3$	91% $((4d^2_-)_2(4d^4)_2)_3$	305.09	[304.0]
	$4d^6[23]_1$	45% $^3D_1$	90% $((4d^2_-)_2(4d^4)_2)_1$	315.32	[310.0]
	$4d^6[24]_2$	32% $^3F_2$	73% $((4d^2_-)_2(4d^4)_2)_2$	325.07	[313.0]
	$4d^6[25]_4$	53% $^1G_4$	63% $((4d^2_-)_2(4d^4)_2)_4$	325.26	[316.0]
	$4d^6[26]_2$	68% $^3F_2$	60% $((4d^2_-)_2(4d^4)_0)_2$	359.51	[347.0]
	$4d^6[27]_4$	52% $^3F_4$	77% $((4d^2_-)_0(4d^4)_4)_4$	372.36	[359.0]
	$4d^6[28]_1$	48% $^3P_1$	96% $((4d_-)_{3/2}(4d^5)_{5/2})_1$	407.40	[413.0]
	$4d^6[29]_2$	66% $^1D_2$	53% $((4d^2_-)_0(4d^4)_2)_2$	430.14	[387.0]
	$4d^6[30]_4$	44% $^1G_4$	92% $((4d_-)_{3/2}(4d^5)_{5/2})_4$	452.80	[440.0]

Table 2. (Continued.)

Ion	Label	*LS* purity	*jj* purity	$E_{\rm MCDF}$[a] (10^3 cm^{-1})	$E_{\rm NIST}$[b] (10^3 cm^{-1})
	$4d^6[31]_2$	25% $^3P_2$	92% $((4d_-)_{3/2}(4d^5)_{5/2})_2$	467.58	[460.0]
	$4d^6[32]_0$	37% $^1S_0$	69% $((4d^2_-)_0(4d^4)_0)_0$	474.94	[421.0]
	$4d^6[33]_3$	39% $^3F_3$	94% $((4d_-)_{3/2}(4d^5)_{5/2})_3$	473.82	[467.0]
	$4d^6[34]_0$	42% $^3P_0$	86% $(4d^6)_0$	592.01	[577.0]
W^{33+}	$4d^5[1]_{5/2}$	28% $^4P_{5/2}$	90% $((4d^4_-)_0(4d)_{5/2})_{5/2}$	0.00	0.0
	$4d^5[2]_{5/2}$	38% $^6S_{5/2}$	67% $((4d^3_-)_{3/2}(4d^2)_4)_{5/2}$	102.17	[105.0]
	$4d^5[3]_{7/2}$	35% $^4G_{7/2}$	83% $((4d^3_-)_{3/2}(4d^2)_4)_{7/2}$	142.23	141.61
	$4d^5[4]_{3/2}$	40% $^4D_{3/2}$	86% $((4d^3_-)_{3/2}(4d^2)_2)_{3/2}$	144.92	144.43
	$4d^5[5]_{11/2}$	40% $^2H_{11/2}$	96% $((4d^3_-)_{3/2}(4d^2)_4)_{11/2}$	151.05	
	$4d^5[6]_{9/2}$	34% $^4G_{9/2}$	93% $((4d^3_-)_{3/2}(4d^2)_4)_{9/2}$	163.33	
	$4d^5[7]_{5/2}$	32% $^4D_{5/2}$	77% $((4d^3_-)_{3/2}(4d^2)_2)_{5/2}$	170.76	
	$4d^5[8]_{1/2}$	47% $^4P_{1/2}$	85% $((4d^3_-)_{3/2}(4d^2)_2)_{1/2}$	176.63	
	$4d^5[9]_{7/2}$	27% $^2F_{7/2}$	79% $((4d^3_-)_{3/2}(4d^2)_2)_{7/2}$	187.48	
	$4d^5[10]_{3/2}$	30% $^2D_{3/2}$	73% $((4d^3_-)_{3/2}(4d^2)_0)_{3/2}$	230.41	
	$4d^5[11]_{5/2}$	26% $^6S_{5/2}$	61% $((4d^2_-)_2(4d^3)_{9/2})_{5/2}$	242.39	246.199
	$4d^5[12]_{7/2}$	51% $^4D_{7/2}$	89% $((4d^2_-)_2(4d^3)_{9/2})_{7/2}$	267.05	
	$4d^5[13]_{11/2}$	51% $^2I_{11/2}$	96% $((4d^2_-)_2(4d^3)_{9/2})_{11/2}$	273.81	
	$4d^5[14]_{9/2}$	56% $^4G_{9/2}$	93% $((4d^2_-)_2(4d^3)_{9/2})_{9/2}$	278.40	
	$4d^5[15]_{1/2}$	75% $^4D_{1/2}$	89% $((4d^2_-)_2(4d^3)_{3/2})_{1/2}$	285.24	
	$4d^5[16]_{3/2}$	52% $^4P_{3/2}$	66% $((4d^2_-)_2(4d^3)_{5/2})_{3/2}$	291.42	
	$4d^5[17]_{13/2}$	86% $^2I_{13/2}$	99% $((4d^2_-)_2(4d^3)_{9/2})_{13/2}$	293.50	
	$4d^5[18]_{5/2}$	40% $^2F_{5/2}$	74% $((4d^2_-)_2(4d^3)_{3/2})_{5/2}$	297.25	
	$4d^5[19]_{9/2}$	51% $^2H_{9/2}$	50% $((4d^2_-)_0(4d^3)_{9/2})_{9/2}$	316.54	
	$4d^5[20]_{7/2}$	61% $^2G_{7/2}$	90% $((4d^2_-)_2(4d^3)_{3/2})_{7/2}$	323.69	
	$4d^5[21]_{5/2}$	61% $^4F_{5/2}$	93% $((4d^2_-)_2(4d^3)_{5/2})_{5/2}$	326.38	
	$4d^5[22]_{3/2}$	69% $^2D_{3/2}$	76% $((4d^2_-)_2(4d^3)_{3/2})_{3/2}$	331.72	
	$4d^5[23]_{1/2}$	36% $^4P_{1/2}$	69% $((4d^2_-)_2(4d^3)_{5/2})_{1/2}$	346.48	
	$4d^5[24]_{7/2}$	42% $^2G_{7/2}$	91% $((4d^2_-)_2(4d^3)_{5/2})_{7/2}$	349.24	
	$4d^5[25]_{9/2}$	69% $^2G_{9/2}$	48% $((4d^2_-)_2(4d^3)_{5/2})_{9/2}$	375.10	
	$4d^5[26]_{5/2}$	33% $^4P_{5/2}$	59% $((4d_-)_{3/2}(4d^4)_4)_{5/2}$	403.81	
	$4d^5[27]_{3/2}$	72% $^2P_{3/2}$	67% $((4d^2_-)_0(4d^3)_{3/2})_{3/2}$	420.69	
	$4d^5[28]_{5/2}$	42% $^2D_{5/2}$	66% $((4d^2_-)_0(4d^3)_{5/2})_{5/2}$	428.76	
	$4d^5[29]_{7/2}$	30% $^4F_{7/2}$	89% $((4d_-)_{3/2}(4d^4)_4)_{7/2}$	433.80	
	$4d^5[30]_{3/2}$	28% $^4D_{3/2}$	83% $((4d_-)_{3/2}(4d^4)_2)_{3/2}$	444.07	
	$4d^5[31]_{11/2}$	56% $^2H_{11/2}$	97% $((4d_-)_{3/2}(4d^4)_4)_{11/2}$	444.26	
	$4d^5[32]_{9/2}$	34% $^2G_{9/2}$	92% $((4d_-)_{3/2}(4d^4)_4)_{9/2}$	465.66	
	$4d^5[33]_{5/2}$	36% $^2D_{5/2}$	66% $((4d_-)_{3/2}(4d^4)_2)_{5/2}$	477.76	
	$4d^5[34]_{7/2}$	43% $^2G_{7/2}$	85% $((4d_-)_{3/2}(4d^4)_2)_{7/2}$	488.64	
	$4d^5[35]_{1/2}$	59% $^2P_{1/2}$	84% $((4d_-)_{3/2}(4d^4)_2)_{1/2}$	514.63	
	$4d^5[36]_{3/2}$	51% $^2D_{3/2}$	80% $((4d_-)_{3/2}(4d^4)_0)_{3/2}$	561.80	
	$4d^5[37]_{5/2}$	33% $^2D_{5/2}$	89% $(4d^5)_{5/2}$	601.88	
W^{34+}	$4d^4[1]_0$	34% $^3P_0$	96% $(4d^4_-)_0$	0.00	0.0
	$4d^4[2]_1$	61% $^5D_1$	96% $((4d^3_-)_{3/2}(4d)_{5/2})_1$	115.88	116.87
	$4d^4[3]_2$	46% $^5D_2$	85% $((4d^3_-)_{3/2}(4d)_{5/2})_2$	158.66	[162.0]
	$4d^4[4]_4$	22% $^3H_4$	96% $((4d^3_-)_{3/2}(4d)_{5/2})_4$	158.51	[159.0]
	$4d^4[5]_3$	26% $^5D_3$	89% $((4d^3_-)_{3/2}(4d)_{5/2})_3$	171.22	[173.0]
	$4d^4[6]_0$	63% $^5D_0$	86% $((4d^2_-)_2(4d^2)_2)_0$	260.65	263.80
	$4d^4[7]_2$	41% $^5D_2$	62% $((4d^2_-)_2(4d^2)_4)_2$	268.17	267.84
	$4d^4[8]_4$	39% $^3H_4$	71% $((4d^2_-)_2(4d^2)_4)_4$	272.76	274.67
	$4d^4[9]_3$	46% $^5D_3$	70% $((4d^2_-)_2(4d^2)_4)_3$	277.05	[283.0]
	$4d^4[10]_5$	67% $^3H_5$	98% $((4d^2_-)_2(4d^2)_4)_5$	294.49	294.75
	$4d^4[11]_1$	39% $^3P_1$	92% $((4d^2_-)_2(4d^2)_2)_1$	302.04	305.48
	$4d^4[12]_6$	50% $^3H_6$	97% $((4d^2_-)_2(4d^2)_4)_6$	306.78	[311.0]
	$4d^4[13]_3$	43% $^3F_3$	80% $((4d^2_-)_2(4d^2)_2)_3$	317.45	[319.0]
	$4d^4[14]_4$	56% $^3G_4$	71% $((4d^2_-)_2(4d^2)_2)_4$	319.06	[318.0]
	$4d^4[15]_2$	33% $^3D_2$	77% $((4d^2_-)_2(4d^2)_2)_2$	321.90	[323.0]
	$4d^4[16]_2$	45% $^3F_2$	61% $((4d^2_-)_2(4d^2)_0)_2$	360.33	[355.0]
	$4d^4[17]_4$	37% $^3F_4$	67% $((4d^2_-)_0(4d^2)_4)_4$	373.77	[363.0]
	$4d^4[18]_2$	33% $^1D_2$	58% $((4d^2_-)_0(4d^2)_2)_2$	409.18	[388.0]
	$4d^4[19]_4$	28% $^5D_4$	76% $((4d_-)_{3/2}(4d^3)_{9/2})_4$	422.90	[426.0]
	$4d^4[20]_3$	35% $^3F_3$	67% $((4d_-)_{3/2}(4d^3)_{9/2})_3$	423.56	[430.0]

Table 2. (Continued.)

Ion	Label	*LS* purity	*jj* purity	E_{MCDF}[a] (10^3 cm^{-1})	E_{NIST}[b] (10^3 cm^{-1})
	$4d^4[21]_1$	54% $^3D_1$	72% $((4d_-)_{3/2}(4d^3)_{3/2})_1$	438.27	[443.0]
	$4d^4[22]_0$	54% $^3P_0$	54% $((4d^2_-)_0(4d^2)_0)_0$	444.48	[426.0]
	$4d^4[23]_5$	66% $^3G_5$	98% $((4d_-)_{3/2}(4d^3)_{9/2})_5$	444.13	[449.0]
	$4d^4[24]_6$	50% $^1I_6$	97% $((4d_-)_{3/2}(4d^3)_{9/2})_6$	449.98	[455.0]
	$4d^4[25]_2$	32% $^3F_2$	58% $((4d_-)_{3/2}(4d^3)_{3/2})_2$	468.13	[468.0]
	$4d^4[26]_3$	35% $^3D_3$	56% $((4d_-)_{3/2}(4d^3)_{3/2})_3$	474.88	[475.0]
	$4d^4[27]_0$	71% $^1S_0$	51% $((4d_-)_{3/2}(4d^3)_{3/2})_0$	504.24	[455.0]
	$4d^4[28]_1$	52% $^3P_1$	71% $((4d_-)_{3/2}(4d^3)_{5/2})_1$	517.76	[512.0]
	$4d^4[29]_3$	51% $^3F_3$	71% $((4d_-)_{3/2}(4d^3)_{5/2})_3$	518.59	[512.0]
	$4d^4[30]_4$	60% $^1G_4$	87% $((4d_-)_{3/2}(4d^3)_{5/2})_4$	525.17	[504.0]
	$4d^4[31]_2$	51% $^1D_2$	49% $((4d_-)_{3/2}(4d^3)_{5/2})_2$	534.65	[513.0]
	$4d^4[32]_4$	37% $^3F_4$	94% $(4d^4)_4$	595.56	[597.0]
	$4d^4[33]_2$	38% $^1D_2$	86% $(4d^4)_2$	630.11	[619.0]
	$4d^4[34]_0$	50% $^1S_0$	85% $(4d^4)_0$	710.15	[680.0]
W^{35+}	$4d^3[1]_{3/2}$	49% $^4F_{3/2}$	95% $(4d^3_-)_{3/2}$	0.00	0.0
	$4d^3[2]_{5/2}$	88% $^4F_{5/2}$	87% $((4d^2_-)_2(4d)_{5/2})_{5/2}$	120.83	121.554
	$4d^3[3]_{3/2}$	39% $^4P_{3/2}$	96% $((4d^2_-)_2(4d)_{5/2})_{3/2}$	140.65	140.75
	$4d^3[4]_{7/2}$	45% $^2G_{7/2}$	93% $((4d^2_-)_2(4d)_{5/2})_{7/2}$	153.10	156.41
	$4d^3[5]_{1/2}$	59% $^4P_{1/2}$	98% $((4d^2_-)_2(4d)_{5/2})_{1/2}$	156.62	160.69
	$4d^3[6]_{9/2}$	42% $^2H_{9/2}$	97% $((4d^2_-)_2(4d)_{5/2})_{9/2}$	157.16	[159.5]
	$4d^3[7]_{5/2}$	44% $^4P_{5/2}$	80% $((4d^2_-)_0(4d)_{5/2})_{5/2}$	221.74	[225.9]
	$4d^3[8]_{7/2}$	59% $^4F_{7/2}$	67% $((4d_-)_{3/2}(4d^2)_4)_{7/2}$	272.15	273.25?
	$4d^3[9]_{9/2}$	52% $^4F_{9/2}$	94% $((4d_-)_{3/2}(4d^2)_4)_{9/2}$	286.60	288.57
	$4d^3[10]_{3/2}$	40% $^4P_{3/2}$	88% $((4d_-)_{3/2}(4d^2)_2)_{3/2}$	298.70	299.52?
	$4d^3[11]_{1/2}$	59% $^2P_{1/2}$	98% $((4d_-)_{3/2}(4d^2)_2)_{1/2}$	308.29	312.20?
	$4d^3[12]_{5/2}$	42% $^2D_{5/2}$	86% $((4d_-)_{3/2}(4d^2)_4)_{5/2}$	315.82	318.12?
	$4d^3[13]_{11/2}$	99% $^2H_{11/2}$	99% $((4d_-)_{3/2}(4d^2)_4)_{11/2}$	319.37	322.01?
	$4d^3[14]_{5/2}$	41% $^2D_{5/2}$	93% $((4d_-)_{3/2}(4d^2)_2)_{5/2}$	338.10	[344.0]
	$4d^3[15]_{7/2}$	81% $^2F_{7/2}$	70% $((4d_-)_{3/2}(4d^2)_2)_{7/2}$	344.85	[350.0]
	$4d^3[16]_{3/2}$	64% $^2D_{3/2}$	78% $((4d_-)_{3/2}(4d^2)_0)_{3/2}$	398.54	402.41?
	$4d^3[17]_{9/2}$	52% $^2G_{9/2}$	96% $(4d^3)_{9/2}$	435.13	[438.0]
	$4d^3[18]_{3/2}$	45% $^2D_{3/2}$	87% $(4d^3)_{3/2}$	478.10	[485.0]
	$4d^3[19]_{5/2}$	61% $^2D_{5/2}$	93% $(4d^3)_{5/2}$	509.82	[516.0]
W^{36+}	$4d^2[1]_2$	74% $^3F_2$	98% $(4d^2_-)_2$	0.00	0.0
	$4d^2[2]_0$	73% $^3P_0$	96% $(4d^2_-)_0$	64.79	67.78
	$4d^2[3]_3$	99% $^3F_3$	99% $((4d_-)_{3/2}(4d)_{5/2})_3$	140.67	141.31
	$4d^2[4]_2$	49% $^3P_2$	98% $((4d_-)_{3/2}(4d)_{5/2})_2$	171.19	174.13
	$4d^2[5]_1$	98% $^3P_1$	98% $((4d_-)_{3/2}(4d)_{5/2})_1$	181.39	184.61
	$4d^2[6]_4$	62% $^1G_4$	95% $((4d_-)_{3/2}(4d)_{5/2})_4$	183.00	182.76?
	$4d^2[7]_4$	62% $^3F_4$	95% $(4d^2)_4$	308.40	308.53
	$4d^2[8]_2$	47% $^3P_2$	98% $(4d^2)_2$	328.67	331.48
	$4d^2[9]_0$	73% $^1S_0$	96% $(4d^2)_0$	404.64	[407.0]
W^{37+}	$4d[1]_{3/2}$	99% $^2D_{3/2}$	99% $(4d_-)_{3/2}$	0.00	0.0
	$4d[2]_{5/2}$	99% $^2D_{5/2}$	99% $(4d)_{5/2}$	154.19	154.64
W^{39+}	$4p^5[1]_{3/2}$	99% $^2P_{3/2}$	99% $((4p^2_-)_0(4p^3)_{3/2})_{3/2}$	0.00	0.0
	$4p^5[2]_{1/2}$	98% $^2P_{1/2}$	98% $((4p_-)_{1/2}(4p^4)_0)_{1/2}$	747.29	742.17
W^{40+}	$4p^4[1]_2$	69% $^3P_2$	99% $((4p^2_-)_0(4p^2)_2)_2$	0.00	0.0
	$4p^4[2]_0$	62% $^1S_0$	99% $((4p^2_-)_0(4p^2)_0)_0$	73.25	72.10
	$4p^4[3]_1$	99% $^3P_1$	99% $((4p_-)_{1/2}(4p^3)_{3/2})_1$	740.74	741.50
	$4p^4[4]_2$	69% $^1D_2$	99% $((4p_-)_{1/2}(4p^3)_{3/2})_2$	778.03	777.40
	$4p^4[5]_0$	61% $^3P_0$	98% $(4p^4)_0$	1548.19	[1547.0]
W^{41+}	$4p^3[1]_{3/2}$	46% $^2P_{3/2}$	99% $((4p^2_-)_0(4p)_{3/2})_{3/2}$	0.00	0.0
	$4p^3[2]_{3/2}$	54% $^4S_{3/2}$	99% $((4p_-)_{1/2}(4p^2)_2)_{3/2}$	716.03	719.60
	$4p^3[3]_{5/2}$	99% $^2D_{5/2}$	99% $((4p_-)_{1/2}(4p^2)_2)_{5/2}$	761.33	762.10
	$4p^3[4]_{1/2}$	99% $^2P_{1/2}$	99% $((4p_-)_{1/2}(4p^2)_0)_{1/2}$	818.73	[802.0]
	$4p^3[5]_{3/2}$	52% $^2P_{3/2}$	98% $(4p^3)_{3/2}$	1542.64	[1528.0]
W^{42+}	$4p^2[1]_0$	70% $^3P_0$	99% $(4p^2_-)_0$	0.00	0.0
	$4p^2[2]_1$	99% $^3P_1$	99% $((4p_-)_{1/2}(4p)_{3/2})_1$	736.10	738.28

Table 2. (Continued.)

Ion	Label	*LS* purity	*jj* purity	E_{MCDF}[a] (10^3 cm^{-1})	E_{NIST}[b] (10^3 cm^{-1})
	$4p^2[3]_2$	63% $^1D_2$	99% $((4p_-)_{1/2}(4p)_{3/2})_2$	771.71	772.74
	$4p^2[4]_2$	63% $^3P_2$	99% $(4p^2)_2$	1534.70	[1535.0]
	$4p^2[5]_0$	69% $^1S_0$	98% $(4p^2)_0$	1612.30	[1609.0]
W^{43+}	$4p[1]_{1/2}$	99% $^2P_{1/2}$	99% $(4p_-)_{1/2}$	0.00	0.0
	$4p[2]_{3/2}$	99% $^2P_{3/2}$	99% $(4p)_{3/2}$	790.71	791.83

[a] This work.

[b] From the latest NIST compilation (Ralchenko *et al* 2011b). The values between parentheses were calculated by Kramida and Shirai (2009) using parametric fitting of Cowan's code. Other values were determined experimentally.

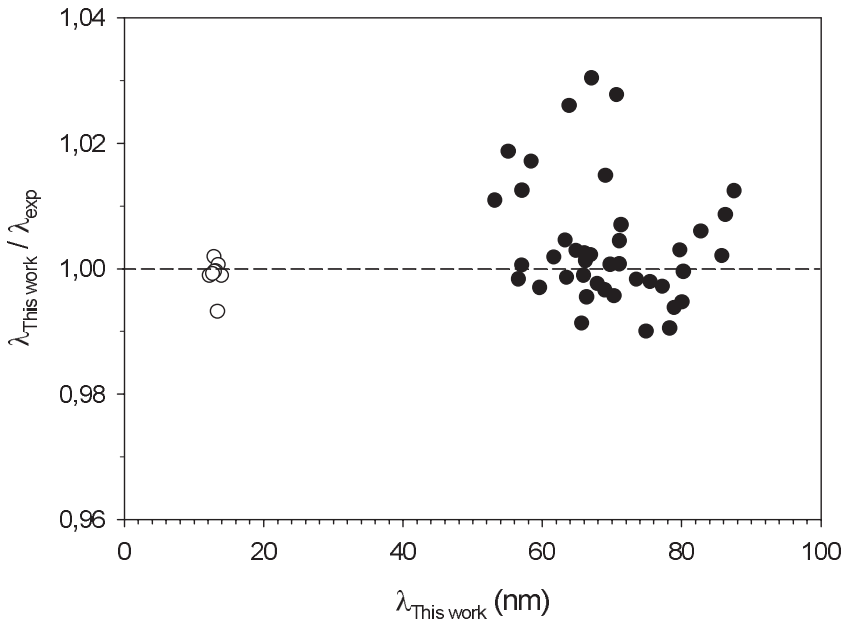

Figure 1. Comparison between calculated wavelengths as obtained in the present work ($\lambda_{This\ work}$) and experimental values (λ_{exp}) published by Radtke *et al* (2007) for magnetic dipole (M1) lines within the $4p^k$ (open circles) and $4d^k$ (full circles) ground configurations of tungsten ions from W^{29+} to W^{43+}.

types of radiations appear for forbidden lines within the $4p^k$ configurations.

Available experimental wavelengths are also given in table 3 for comparison. These values were determined by Radtke *et al* (2007) who used high-resolution x-ray and extreme ultraviolet tungsten spectra produced in an EBIT source. Among the emission lines from highly charged tungsten ions observed by these authors, 41 were identified as being due to forbidden transitions within the $4d^k$ ground configurations of W^{29+} through W^{37+}, while 8 lines were identified as arising from the $4p^k$ ground configurations of W^{39+} through W^{43+}. In general, our theoretical results agree rather well with the experimental wavelengths, the mean ratio $\lambda_{This\ work}/\lambda_{exp}$ being found equal to 1.003 ± 0.009 where the uncertainty represents the standard deviation of the mean. This is illustrated in figure 1 where this ratio is shown as a function of $\lambda_{This\ work}$ for each available measured wavelength. However, when looking at this figure in more detail, one can note that the agreement with experimental data is better for forbidden lines within $4p^k$ ($\lambda_{This\ work}/\lambda_{exp}$ = 0.999 ± 0.003) than for those within the $4d^k$ ($\lambda_{This\ work}/\lambda_{exp}$ = 1.004 ± 0.010) ground configurations, the scattering being much larger for the latter than for the former ones. This was already mentioned by Jonauskas *et al* (2010) who critically evaluated the line identifications by Radtke *et al* (2007) for the $4d^k$ transitions in multicharged tungsten ions thanks to detailed comparisons of experimental wavelengths with values computed using different theoretical approaches. In this study, new interpretations of some lines were proposed that allowed the large theory–experiment deviations that existed in the previous data to be removed. Questionable experimental wavelengths or line identifications in Radtke *et al* (2007) were also highlighted by Jonauskas *et al* (2010) for five transitions in W^{30+} (λ_{exp} = 57.041, 65.092, 68.757, 79.031 and 79.421 nm), two transitions in W^{35+} (λ_{exp} = 75.664 and 82.268 nm) and one transition in W^{36+} (λ_{exp} = 52.619 nm).

In figure 2, we compare the wavelengths calculated in this work for forbidden lines in the $4d^k$ configurations with those computed by Radtke *et al* (2007) using the Hebrew University Lawrence Livermore Atomic Code (HULLAC) package and with those calculated by Jonauskas *et al* (2010) using the GRASP and FAC codes including only six configurations, i.e. $4s^24p^64d^k + 4s^24p^64d^{k-2}4f^2 + 4s^24p^44d^{k+2} + 4s^24p^54d^k4f + 4s^24p^54d^k4f^2 + 4s4p^54d^{k+1}4f$ (GRASP6, FAC6) and using

Table 3. Forbidden transitions within the $4p^k$ and $4d^k$ ground configurations of tungsten ions. Only transitions with A-values greater than 10^4 s^{-1} are given except for a few experimentally observed lines. $X(Y)$ stands for $X \times 10^Y$.

Ion	Lower level[a]	Upper level[a]	λ_{exp}[b] (nm)	λ_{MCDF}[c] (nm)	Type	A_{MCDF}[c] (s^{-1})	A_{prev} (s^{-1})
W^{29+}	$4d^9[1]_{5/2}$	$4d^9[2]_{3/2}$	75.664	75.506	M1	3.74(4)	3.72(4)[d]
W^{30+}	$4d^8[6]_1$	$4d^8[9]_0$		54.347	M1	1.39(5)	
	$4d^8[1]_4$	$4d^8[7]_4$	57.041	57.072	M1	1.71(4)	1.69(4)[d]
	$4d^8[4]_3$	$4d^8[8]_2$	65.092	67.070	M1	6.52(4)	6.49(4)[d]
	$4d^8[2]_2$	$4d^8[6]_1$	68.757	70.664	M1	2.54(4)	2.51(4)[d]
	$4d^8[2]_2$	$4d^8[5]_2$	79.031	78.280	M1	2.83(4)	2.81(4)[d]
	$4d^8[1]_4$	$4d^8[4]_3$	79.421	78.926	M1	4.71(4)	4.68(4)[d]
	$4d^8[5]_2$	$4d^8[8]_2$		82.334	M1	1.80(4)	
W^{31+}	$4d^7[7]_{5/2}$	$4d^7[18]_{5/2}$		43.498	M1	3.07(4)	
	$4d^7[3]_{5/2}$	$4d^7[12]_{3/2}$		49.093	M1	1.66(4)	
	$4d^7[4]_{7/2}$	$4d^7[17]_{7/2}$		52.145	M1	1.79(4)	
	$4d^7[11]_{5/2}$	$4d^7[18]_{5/2}$		55.728	M1	2.75(4)	
	$4d^7[13]_{5/2}$	$4d^7[19]_{3/2}$		59.052	M1	1.05(4)	
	$4d^7[5]_{9/2}$	$4d^7[17]_{7/2}$		60.234	M1	2.49(4)	
	$4d^7[14]_{3/2}$	$4d^7[19]_{3/2}$		62.987	M1	5.05(4)	
	$4d^7[5]_{9/2}$	$4d^7[16]_{9/2}$		64.360	M1	3.53(4)	
	$4d^7[3]_{5/2}$	$4d^7[11]_{5/2}$		65.107	M1	1.19(4)	
	$4d^7[4]_{7/2}$	$4d^7[13]_{5/2}$		65.969	M1	9.63(4)	
	$4d^7[1]_{9/2}$	$4d^7[5]_{9/2}$	66.676	66.373	M1	3.55(4)	3.49(4)[d]
	$4d^7[6]_{3/2}$	$4d^7[15]_{1/2}$		67.058	M1	1.54(4)	
	$4d^7[8]_{1/2}$	$4d^7[15]_{1/2}$		72.771	M1	5.21(4)	
	$4d^7[6]_{3/2}$	$4d^7[14]_{3/2}$		74.956	M1	3.69(4)	
	$4d^7[12]_{3/2}$	$4d^7[18]_{5/2}$		77.313	M1	1.55(4)	
	$4d^7[2]_{3/2}$	$4d^7[8]_{1/2}$		77.508	M1	3.74(4)	
	$4d^7[9]_{11/2}$	$4d^7[16]_{9/2}$		77.765	M1	1.89(4)	
	$4d^7[7]_{5/2}$	$4d^7[14]_{3/2}$		78.096	M1	4.07(4)	
	$4d^7[1]_{9/2}$	$4d^7[4]_{7/2}$	80.488	80.060	M1	5.00(4)	4.97(4)[d]
	$4d^7[6]_{3/2}$	$4d^7[13]_{5/2}$		81.412	M1	1.06(4)	
	$4d^7[2]_{3/2}$	$4d^7[7]_{5/2}$		81.517	M1	1.37(4)	
	$4d^7[2]_{3/2}$	$4d^7[6]_{3/2}$		85.244	M1	2.14(4)	
	$4d^7[3]_{5/2}$	$4d^7[7]_{5/2}$		96.956	M1	1.07(4)	
	$4d^7[3]_{5/2}$	$4d^7[6]_{3/2}$		102.270	M1	2.04(4)	
W^{32+}	$4d^6[13]_1$	$4d^6[32]_0$		37.873	M1	7.09(4)	
	$4d^6[10]_3$	$4d^6[29]_2$		38.865	M1	1.29(4)	
	$4d^6[13]_1$	$4d^6[29]_2$		45.612	M1	1.79(4)	
	$4d^6[16]_2$	$4d^6[31]_2$		46.244	M1	1.47(4)	
	$4d^6[4]_3$	$4d^6[24]_2$		47.347	M1	1.10(4)	
	$4d^6[15]_3$	$4d^6[29]_2$		48.332	M1	1.42(4)	
	$4d^6[18]_4$	$4d^6[33]_3$		50.070	M1	1.10(4)	
	$4d^6[12]_2$	$4d^6[28]_1$		50.586	M1	1.16(4)	
	$4d^6[19]_3$	$4d^6[33]_3$		52.752	M1	4.59(4)	
	$4d^6[6]_1$	$4d^6[23]_1$		53.368	M1	2.57(4)	
	$4d^6[28]_1$	$4d^6[34]_0$		54.168	M1	2.70(5)	
	$4d^6[19]_3$	$4d^6[31]_2$		54.549	M1	5.01(4)	
	$4d^6[18]_4$	$4d^6[30]_4$		55.960	M1	7.30(4)	
	$4d^6[7]_5$	$4d^6[25]_4$		57.411	M1	3.14(4)	
	$4d^6[1]_4$	$4d^6[10]_3$		57.856	M1	1.86(4)	
	$4d^6[4]_3$	$4d^6[19]_3$		58.690	M1	3.60(4)	
	$4d^6[22]_3$	$4d^6[33]_3$		59.267	M1	1.65(4)	
	$4d^6[20]_5$	$4d^6[30]_4$		60.755	M1	4.33(4)	
	$4d^6[5]_4$	$4d^6[19]_3$		62.628	M1	2.88(4)	
	$4d^6[14]_4$	$4d^6[27]_4$		62.909	M1	1.68(4)	
	$4d^6[9]_2$	$4d^6[24]_2$		63.531	M1	2.42(4)	
	$4d^6[16]_2$	$4d^6[28]_1$		64.076	M1	1.50(5)	
	$4d^6[23]_1$	$4d^6[31]_2$		65.676	M1	3.49(4)	
	$4d^6[10]_3$	$4d^6[24]_2$		65.690	M1	1.36(4)	
	$4d^6[1]_4$	$4d^6[7]_5$	66.108	66.192	M1	9.28(3)	9.20(3)[d]
	$4d^6[12]_2$	$4d^6[26]_2$		66.754	M1	2.79(4)	
	$4d^6[15]_3$	$4d^6[27]_4$		66.869	M1	2.19(4)	
	$4d^6[5]_4$	$4d^6[18]_4$		66.882	M1	7.09(4)	

Table 3. (Continued.)

Ion	Lower level[a]	Upper level[a]	λ_{exp}[b] (nm)	λ_{MCDF}[c] (nm)	Type	A_{MCDF}[c] (s^{-1})	A_{prev} (s^{-1})
	$4d^6[8]_6$	$4d^6[21]_6$	66.819	66.969	M1	2.20(4)	2.18(4)[d]
	$4d^6[13]_1$	$4d^6[26]_2$		67.289	M1	1.37(4)	
	$4d^6[25]_4$	$4d^6[33]_3$		67.310	M1	1.31(4)	
	$4d^6[22]_3$	$4d^6[30]_4$		67.702	M1	2.14(4)	
	$4d^6[2]_2$	$4d^6[9]_2$		68.530	M1	3.02(4)	
	$4d^6[17]_0$	$4d^6[28]_1$		68.933	M1	3.62(4)	
	$4d^6[24]_2$	$4d^6[31]_2$		70.174	M1	2.13(4)	
	$4d^6[3]_0$	$4d^6[13]_1$		71.030	M1	1.75(4)	
	$4d^6[4]_3$	$4d^6[16]_2$		72.747	M1	7.59(4)	
	$4d^6[9]_2$	$4d^6[22]_3$		72.768	M1	1.40(4)	
	$4d^6[7]_5$	$4d^6[20]_5$		72.923	M1	1.39(4)	
	$4d^6[15]_3$	$4d^6[26]_2$		73.152	M1	2.35(4)	
	$4d^6[8]_6$	$4d^6[20]_5$		74.095	M1	2.70(4)	
	$4d^6[6]_1$	$4d^6[17]_0$		74.410	M1	1.15(5)	
	$4d^6[10]_3$	$4d^6[22]_3$		75.615	M1	2.27(4)	
	$4d^6[1]_4$	$4d^6[5]_4$	80.303	80.266	M1	4.15(4)	4.07(4)[d]
	$4d^6[6]_1$	$4d^6[16]_2$		81.042	M1	2.13(4)	
	$4d^6[7]_5$	$4d^6[18]_4$		81.283	M1	1.33(4)	
	$4d^6[9]_2$	$4d^6[19]_3$		85.773	M1	1.04(4)	
	$4d^6[26]_2$	$4d^6[33]_3$		87.483	M1	1.64(4)	
	$4d^6[1]_4$	$4d^6[4]_3$		87.820	M1	3.23(4)	3.18(4)[d]
	$4d^6[11]_0$	$4d^6[23]_1$		89.043	M1	1.28(4)	
	$4d^6[2]_2$	$4d^6[6]_1$		94.172	M1	4.00(4)	
	$4d^6[13]_1$	$4d^6[23]_1$		95.772	M1	1.07(4)	
W^{33+}	$4d^5[16]_{3/2}$	$4d^5[36]_{3/2}$		36.984	M1	1.23(4)	
	$4d^5[15]_{1/2}$	$4d^5[35]_{1/2}$		43.594	M1	1.43(4)	
	$4d^5[16]_{3/2}$	$4d^5[35]_{1/2}$		44.800	M1	2.10(4)	
	$4d^5[12]_{7/2}$	$4d^5[33]_{5/2}$		47.458	M1	2.67(4)	
	$4d^5[14]_{9/2}$	$4d^5[34]_{7/2}$		47.564	M1	1.45(4)	
	$4d^5[11]_{5/2}$	$4d^5[30]_{3/2}$		49.583	M1	1.34(4)	
	$4d^5[4]_{3/2}$	$4d^5[23]_{1/2}$		49.613	M1	3.91(4)	
	$4d^5[12]_{7/2}$	$4d^5[32]_{9/2}$		50.350	M1	1.85(4)	
	$4d^5[10]_{3/2}$	$4d^5[28]_{5/2}$		50.418	M1	1.49(4)	
	$4d^5[26]_{5/2}$	$4d^5[37]_{5/2}$		50.487	M1	1.07(5)	
	$4d^5[13]_{11/2}$	$4d^5[32]_{9/2}$		52.124	M1	1.28(4)	
	$4d^5[2]_{5/2}$	$4d^5[16]_{3/2}$		52.842	M1	3.50(4)	
	$4d^5[9]_{7/2}$	$4d^5[25]_{9/2}$		53.300	M1	1.70(4)	
	$4d^5[11]_{5/2}$	$4d^5[28]_{5/2}$		53.658	M1	1.63(4)	
	$4d^5[6]_{9/2}$	$4d^5[24]_{7/2}$		53.788	M1	1.72(4)	
	$4d^5[3]_{7/2}$	$4d^5[21]_{5/2}$		54.304	M1	2.83(4)	
	$4d^5[4]_{3/2}$	$4d^5[21]_{5/2}$		55.110	M1	1.23(4)	
	$4d^5[18]_{5/2}$	$4d^5[33]_{5/2}$		55.397	M1	2.49(4)	
	$4d^5[3]_{7/2}$	$4d^5[19]_{9/2}$		57.370	M1	1.25(4)	
	$4d^5[13]_{11/2}$	$4d^5[31]_{11/2}$		58.667	M1	5.90(4)	
	$4d^5[8]_{1/2}$	$4d^5[23]_{1/2}$		58.875	M1	2.20(4)	
	$4d^5[23]_{1/2}$	$4d^5[35]_{1/2}$		59.471	M1	4.53(4)	
	$4d^5[29]_{7/2}$	$4d^5[37]_{5/2}$		59.493	M1	5.82(4)	
	$4d^5[12]_{7/2}$	$4d^5[29]_{7/2}$		59.970	M1	3.58(4)	
	$4d^5[14]_{9/2}$	$4d^5[31]_{11/2}$		60.290	M1	1.73(4)	
	$4d^5[5]_{11/2}$	$4d^5[19]_{9/2}$		60.429	M1	1.38(4)	
	$4d^5[2]_{5/2}$	$4d^5[12]_{7/2}$		60.653	M1	1.20(4)	
	$4d^5[21]_{5/2}$	$4d^5[34]_{7/2}$		61.628	M1	1.96(4)	
	$4d^5[9]_{7/2}$	$4d^5[24]_{7/2}$		61.818	M1	1.61(4)	
	$4d^5[11]_{5/2}$	$4d^5[26]_{5/2}$		61.948	M1	1.12(5)	
	$4d^5[7]_{5/2}$	$4d^5[22]_{3/2}$		62.126	M1	1.09(4)	
	$4d^5[6]_{9/2}$	$4d^5[20]_{7/2}$		62.358	M1	1.11(4)	
	$4d^5[15]_{1/2}$	$4d^5[30]_{3/2}$		62.961	M1	4.74(4)	
	$4d^5[30]_{3/2}$	$4d^5[37]_{5/2}$		63.367	M1	4.75(4)	
	$4d^5[14]_{9/2}$	$4d^5[29]_{7/2}$		64.350	M1	4.10(4)	
	$4d^5[3]_{7/2}$	$4d^5[18]_{5/2}$		64.510	M1	1.69(4)	
	$4d^5[6]_{9/2}$	$4d^5[19]_{9/2}$		65.271	M1	4.14(4)	

Table 3. (Continued.)

Ion	Lower level[a]	Upper level[a]	λ_{exp}[b] (nm)	λ_{MCDF}[c] (nm)	Type	A_{MCDF}[c] (s^{-1})	A_{prev} (s^{-1})
	$4d^5[16]_{3/2}$	$4d^5[30]_{3/2}$		65.507	M1	5.99(4)	
	$4d^5[17]_{13/2}$	$4d^5[31]_{11/2}$		66.331	M1	1.35(4)	
	$4d^5[19]_{9/2}$	$4d^5[32]_{9/2}$		67.061	M1	3.04(4)	
	$4d^5[18]_{5/2}$	$4d^5[30]_{3/2}$		68.108	M1	1.95(4)	
	$4d^5[4]_{3/2}$	$4d^5[16]_{3/2}$		68.262	M1	4.87(4)	
	$4d^5[22]_{3/2}$	$4d^5[33]_{5/2}$		68.475	M1	2.19(4)	
	$4d^5[1]_{5/2}$	$4d^5[4]_{3/2}$	69.236	69.002	M1	5.63(4)	5.57(4)[d]
	$4d^5[1]_{5/2}$	$4d^5[3]_{7/2}$	70.618	70.308	M1	2.14(4)	2.12(4)[d]
	$4d^5[20]_{7/2}$	$4d^5[32]_{9/2}$		70.442	M1	1.16(4)	
	$4d^5[27]_{3/2}$	$4d^5[36]_{3/2}$		70.867	M1	1.12(4)	
	$4d^5[4]_{3/2}$	$4d^5[15]_{1/2}$		71.265	M1	4.04(4)	
	$4d^5[2]_{5/2}$	$4d^5[11]_{5/2}$	70.822	71.318	M1	9.16(4)	9.03(4)[d]
	$4d^5[24]_{7/2}$	$4d^5[34]_{7/2}$		71.738	M1	1.30(4)	
	$4d^5[9]_{7/2}$	$4d^5[21]_{5/2}$		71.995	M1	2.01(4)	
	$4d^5[12]_{7/2}$	$4d^5[26]_{5/2}$		73.116	M1	3.08(4)	
	$4d^5[18]_{5/2}$	$4d^5[29]_{7/2}$		73.233	M1	1.93(4)	
	$4d^5[3]_{7/2}$	$4d^5[14]_{9/2}$		73.440	M1	1.87(4)	
	$4d^5[28]_{5/2}$	$4d^5[36]_{3/2}$		75.161	M1	1.90(4)	
	$4d^5[5]_{11/2}$	$4d^5[14]_{9/2}$		78.528	M1	1.23(4)	
	$4d^5[7]_{5/2}$	$4d^5[18]_{5/2}$		79.058	M1	2.31(4)	
	$4d^5[3]_{7/2}$	$4d^5[12]_{7/2}$		80.119	M1	1.87(4)	
	$4d^5[5]_{11/2}$	$4d^5[13]_{11/2}$		81.465	M1	3.09(4)	
	$4d^5[7]_{5/2}$	$4d^5[16]_{3/2}$		82.877	M1	1.56(4)	
	$4d^5[25]_{9/2}$	$4d^5[34]_{7/2}$		88.072	M1	1.29(4)	
	$4d^5[8]_{1/2}$	$4d^5[15]_{1/2}$		92.070	M1	2.29(4)	
	$4d^5[6]_{9/2}$	$4d^5[12]_{7/2}$		96.417	M1	1.20(4)	
	$4d^5[1]_{5/2}$	$4d^5[2]_{5/2}$		97.874	M1	3.97(4)	3.90(4)[d]
	$4d^5[10]_{3/2}$	$4d^5[21]_{5/2}$		104.200	M1	1.01(4)	
W^{34+}	$4d^4[2]_1$	$4d^4[22]_0$		30.432	M1	1.73(4)	
	$4d^4[21]_1$	$4d^4[34]_0$		36.781	M1	6.76(4)	
	$4d^4[9]_3$	$4d^4[31]_2$		38.820	M1	1.00(4)	
	$4d^4[7]_2$	$4d^4[28]_1$		40.066	M1	2.11(4)	
	$4d^4[11]_1$	$4d^4[31]_2$		42.992	M1	1.29(4)	
	$4d^4[10]_5$	$4d^4[30]_4$		43.350	M1	2.91(4)	
	$4d^4[11]_1$	$4d^4[28]_1$		46.358	M1	1.38(4)	
	$4d^4[13]_3$	$4d^4[30]_4$		48.141	M1	2.12(4)	
	$4d^4[20]_3$	$4d^4[33]_2$		48.414	M1	4.36(4)	
	$4d^4[5]_3$	$4d^4[17]_4$		49.372	M1	1.77(4)	
	$4d^4[11]_1$	$4d^4[27]_0$		49.458	M1	3.90(4)	
	$4d^4[8]_4$	$4d^4[26]_3$		49.476	M1	1.03(4)	
	$4d^4[3]_2$	$4d^4[16]_2$		49.587	M1	1.61(4)	
	$4d^4[28]_1$	$4d^4[34]_0$		51.977	M1	1.66(5)	
	$4d^4[21]_1$	$4d^4[33]_2$		52.126	M1	6.23(4)	
	$4d^4[9]_3$	$4d^4[25]_2$		52.334	M1	2.94(4)	
	$4d^4[5]_3$	$4d^4[16]_2$		52.882	M1	5.60(4)	
	$4d^4[6]_0$	$4d^4[21]_1$		56.299	M1	5.87(4)	
	$4d^4[16]_2$	$4d^4[31]_2$		57.365	M1	2.70(4)	
	$4d^4[19]_4$	$4d^4[32]_4$		57.917	M1	7.77(4)	
	$4d^4[20]_3$	$4d^4[32]_4$		58.141	M1	5.31(4)	
	$4d^4[7]_2$	$4d^4[21]_1$		58.788	M1	6.00(4)	
	$4d^4[11]_1$	$4d^4[25]_2$		60.209	M1	1.52(4)	
	$4d^4[25]_2$	$4d^4[33]_2$		61.736	M1	4.32(4)	
	$4d^4[4]_4$	$4d^4[13]_3$		62.916	M1	2.63(4)	
	$4d^4[16]_2$	$4d^4[29]_3$		63.187	M1	1.81(4)	
	$4d^4[13]_3$	$4d^4[26]_3$		63.520	M1	2.82(4)	
	$4d^4[16]_2$	$4d^4[28]_1$		63.520	M1	2.66(4)	
	$4d^4[10]_5$	$4d^4[24]_6$		64.314	M1	2.80(4)	
	$4d^4[7]_2$	$4d^4[20]_3$		64.351	M1	6.62(4)	
	$4d^4[26]_3$	$4d^4[33]_2$		64.419	M1	1.43(4)	
	$4d^4[15]_2$	$4d^4[26]_3$		65.367	M1	1.32(4)	
	$4d^4[2]_1$	$4d^4[7]_2$	66.240	65.663	M1	6.52(4)	6.45(4)[d]
	$4d^4[23]_5$	$4d^4[32]_4$		66.036	M1	2.05(4)	

Table 3. (Continued.)

Ion	Lower level[a]	Upper level[a]	λ_{exp}[b] (nm)	λ_{MCDF}[c] (nm)	Type	A_{MCDF}[c] (s^{-1})	A_{prev} (s^{-1})
	$4d^4[17]_4$	$4d^4[30]_4$		66.048	M1	2.20(4)	
	$4d^4[13]_3$	$4d^4[25]_2$		66.365	M1	2.93(4)	
	$4d^4[8]_4$	$4d^4[19]_4$		66.605	M1	7.16(4)	
	$4d^4[10]_5$	$4d^4[23]_5$		66.829	M1	1.64(4)	
	$4d^4[9]_3$	$4d^4[20]_3$		68.253	M1	4.42(4)	
	$4d^4[15]_2$	$4d^4[25]_2$		68.382	M1	2.29(4)	
	$4d^4[9]_3$	$4d^4[19]_4$		68.564	M1	2.56(4)	
	$4d^4[17]_4$	$4d^4[29]_3$		69.053	M1	2.63(4)	
	$4d^4[2]_1$	$4d^4[6]_0$	68.060	69.073	M1	1.24(5)	1.23(5)[d]
	$4d^4[3]_2$	$4d^4[11]_1$	69.695	69.742	M1	5.03(4)	4.97(4)[d]
	$4d^4[12]_6$	$4d^4[24]_6$		69.833	M1	2.30(4)	
	$4d^4[11]_1$	$4d^4[22]_0$		70.207	M1	3.08(4)	
	$4d^4[12]_6$	$4d^4[23]_5$		72.809	M1	1.12(4)	
	$4d^4[11]_1$	$4d^4[21]_1$		73.407	M1	2.82(4)	
	$4d^4[4]_4$	$4d^4[10]_5$	73.664	73.538	M1	2.31(4)	2.29(4)[d]
	$4d^4[14]_4$	$4d^4[23]_5$		79.958	M1	2.04(4)	
	$4d^4[3]_2$	$4d^4[9]_3$		84.465	M1	1.89(4)	
	$4d^4[1]_0$	$4d^4[2]_1$	85.563	86.300	M1	4.11(4)	4.08(4)[d]
	$4d^4[4]_4$	$4d^4[8]_4$	86.451	87.525	M1	3.76(4)	3.70(4)[d]
	$4d^4[3]_2$	$4d^4[7]_2$		91.318	M1	1.42(4)	
	$4d^4[18]_2$	$4d^4[28]_1$		92.100	M1	1.49(4)	
	$4d^4[5]_3$	$4d^4[9]_3$		94.494	M1	2.47(4)	
W^{35+}	$4d^3[2]_{5/2}$	$4d^3[16]_{3/2}$		36.009	M1	1.54(4)	
	$4d^3[8]_{7/2}$	$4d^3[19]_{5/2}$		42.075	M1	2.47(4)	
	$4d^3[10]_{3/2}$	$4d^3[19]_{5/2}$		47.365	M1	4.60(4)	
	$4d^3[12]_{5/2}$	$4d^3[19]_{5/2}$		51.546	M1	3.77(4)	
	$4d^3[4]_{7/2}$	$4d^3[15]_{7/2}$		52.149	M1	1.16(4)	
	$4d^3[6]_{9/2}$	$4d^3[15]_{7/2}$		53.278	M1	1.10(4)	
	$4d^3[4]_{7/2}$	$4d^3[14]_{5/2}$		54.053	M1	1.89(4)	
	$4d^3[10]_{3/2}$	$4d^3[18]_{3/2}$		55.741	M1	4.36(4)	
	$4d^3[2]_{5/2}$	$4d^3[10]_{3/2}$		56.223	M1	3.19(4)	
	$4d^3[7]_{5/2}$	$4d^3[16]_{3/2}$	56.654	56.559	M1	3.91(4)	3.90(4)[d]
	$4d^3[3]_{3/2}$	$4d^3[12]_{5/2}$	56.382	57.086	M1	3.64(4)	3.62(4)[d]
	$4d^3[14]_{5/2}$	$4d^3[19]_{5/2}$		58.233	M1	2.65(4)	
	$4d^3[11]_{1/2}$	$4d^3[18]_{3/2}$		58.889	M1	2.66(4)	
	$4d^3[15]_{7/2}$	$4d^3[19]_{5/2}$		60.616	M1	1.54(4)	
	$4d^3[8]_{7/2}$	$4d^3[17]_{9/2}$		61.358	M1	6.26(4)	
	$4d^3[12]_{5/2}$	$4d^3[18]_{3/2}$		61.624	M1	4.08(4)	
	$4d^3[6]_{9/2}$	$4d^3[13]_{11/2}$	61.534	61.646	M1	2.20(4)	2.19(4)[d]
	$4d^3[3]_{3/2}$	$4d^3[10]_{3/2}$	62.985	63.272	M1	6.72(4)	6.67(4)[d]
	$4d^3[1]_{3/2}$	$4d^3[5]_{1/2}$	62.230	63.849	M1	1.39(4)	1.39(4)[d]
	$4d^3[5]_{1/2}$	$4d^3[11]_{1/2}$	66.003	65.933	M1	6.71(4)	6.66(4)[d]
	$4d^3[2]_{5/2}$	$4d^3[8]_{7/2}$	65.920	66.084	M1	7.31(4)	7.27(4)[d]
	$4d^3[9]_{9/2}$	$4d^3[17]_{9/2}$		67.324	M1	4.44(4)	
	$4d^3[5]_{1/2}$	$4d^3[10]_{3/2}$		70.384	M1	1.15(4)	
	$4d^3[1]_{3/2}$	$4d^3[3]_{3/2}$	71.046	71.099	M1	3.72(4)	3.70(4)[d]
	$4d^3[4]_{7/2}$	$4d^3[9]_{9/2}$	75.664	74.906	M1	1.96(4)	1.95(4)[d]
	$4d^3[6]_{9/2}$	$4d^3[9]_{9/2}$	77.476	77.257	M1	3.18(4)	3.15(4)[d]
	$4d^3[1]_{3/2}$	$4d^3[2]_{5/2}$	82.268	82.759	M1	4.53(4)	4.49(4)[d]
	$4d^3[4]_{7/2}$	$4d^3[8]_{7/2}$		83.993	M1	1.64(4)	
	$4d^3[7]_{5/2}$	$4d^3[14]_{5/2}$		85.939	M1	1.43(4)	
W^{36+}	$4d^2[5]_1$	$4d^2[9]_0$		44.793	M1	1.52(5)	1.51(5)[d]
	$4d^2[3]_3$	$4d^2[8]_2$	52.619	53.193	M1	1.27(4)	1.27(4)[d]
	$4d^2[1]_2$	$4d^2[5]_1$	54.120	55.130	M1	3.77(3)	3.76(3)[d]
	$4d^2[1]_2$	$4d^2[4]_2$	57.430	58.414	M1	2.77(4)	2.76(4)[d]
	$4d^2[3]_3$	$4d^2[7]_4$	59.801	59.620	M1	5.95(4)	5.92(4)[d]
	$4d^2[4]_2$	$4d^2[8]_2$	63.589	63.501	M1	4.80(4)	4.77(4)[d]
	$4d^2[5]_1$	$4d^2[8]_2$	68.060	67.899	M1	2.04(4)	2.03(4)[d]
	$4d^2[1]_2$	$4d^2[3]_3$	70.774	71.087	M1	5.39(4)	5.35(4)[d]
	$4d^2[6]_4$	$4d^2[7]_4$	79.509	79.745	M1	1.55(4)	1.55(4)[d]
	$4d^2[2]_0$	$4d^2[5]_1$	85.585	85.761	M1	2.11(4)	2.10(4)[d]

Table 3. (Continued.)

Ion	Lower level[a]	Upper level[a]	λ_{exp}[b] (nm)	λ_{MCDF}[c] (nm)	Type	A_{MCDF}[c] (s^{-1})	A_{prev} (s^{-1})
W^{37+}	$4d[1]_{3/2}$	$4d[2]_{5/2}$	64.668	64.856	M1	3.93(4)	3.97(4)[d]
W^{39+}	$4p^5[1]_{3/2}$	$4p^5[2]_{1/2}$	13.474	13.382	M1+E2	7.65(6)	7.36(6)[e]
W^{40+}	$4p^4[1]_2$	$4p^4[5]_0$		6.459	E2	1.96(4)	
	$4p^4[3]_1$	$4p^4[5]_0$		12.385	M1	1.72(7)	
	$4p^4[1]_2$	$4p^4[4]_2$	12.829	12.853	M1+E2	4.18(6)	3.93(6)[e]
	$4p^4[4]_2$	$4p^4[5]_0$		12.984	E2	8.23(5)	
	$4p^4[1]_2$	$4p^4[3]_1$	13.491	13.500	M1+E2	6.39(6)	6.23(6)[e]
	$4p^4[2]_0$	$4p^4[4]_2$		14.189	E2	4.44(4)	
	$4p^4[2]_0$	$4p^4[3]_1$		14.982	M1	1.97(6)	1.88(6)[e]
W^{41+}	$4p^3[2]_{3/2}$	$4p^3[5]_{3/2}$		12.098	M1+E2	9.17(6)	
	$4p^3[1]_{3/2}$	$4p^3[4]_{1/2}$	12.228	12.214	M1+E2	4.77(6)	4.60(6)[e]
	$4p^3[3]_{5/2}$	$4p^3[5]_{3/2}$		12.799	M1+E2	2.60(6)	
	$4p^3[1]_{3/2}$	$4p^3[3]_{5/2}$	13.139	13.135	M1+E2	1.47(6)	1.21(6)[e]
	$4p^3[4]_{1/2}$	$4p^3[5]_{3/2}$		13.814	M1+E2	1.83(6)	
	$4p^3[1]_{3/2}$	$4p^3[2]_{3/2}$	13.981	13.966	M1+E2	7.05(6)	6.84(6)[e]
W^{42+}	$4p^2[2]_1$	$4p^2[5]_0$		11.413	M1	1.04(7)	
	$4p^2[3]_2$	$4p^2[5]_0$		11.896	E2	6.58(5)	
	$4p^2[2]_1$	$4p^2[4]_2$		12.522	M1+E2	4.37(6)	
	$4p^2[1]_0$	$4p^2[3]_2$	12.964	12.958	E2	1.48(5)	1.40(5)[e]
	$4p^2[3]_2$	$4p^2[4]_2$		13.106	M1+E2	4.34(6)	
	$4p^2[1]_0$	$4p^2[2]_1$		13.585	M1	4.93(6)	4.84(6)[e]
W^{43+}	$4p[1]_{1/2}$	$4p[2]_{3/2}$	12.657	12.647	M1+E2	4.55(6)	4.38(6)[e]

[a] Level designations from table 2.
[b] From Radtke *et al* (2007).
[c] This work.
[d] FAC calculations from Jonauskas *et al* (2010).
[e] Deduced from MCDF oscillator strengths of Fournier (1998).

the FAC code within an extended multiconfiguration basis (FACext) including a number of added configurations ranging from 13 (in W^{37+}) to 34 (in W^{29+}). It is clearly seen from figure 2 that our wavelengths are in much better agreement with the FACext results ($\lambda_{This\ work}/\lambda_{FACext} = 0.999 \pm 0.001$) than with those obtained with HULLAC ($\lambda_{This\ work}/\lambda_{HULLAC} = 0.999 \pm 0.005$), GRASP6 ($\lambda_{This\ work}/\lambda_{GRASP6} = 1.000 \pm 0.005$) and FAC6 ($\lambda_{This\ work}/\lambda_{FAC6} = 1.003 \pm 0.004$) models. It is thus expected that the accuracy for most wavelengths computed in our work is similar to that estimated by Jonauskas *et al* (2010) for their FACext results, i.e. 0.5%.

A very small number of transition probabilities were determined previously for forbidden lines in tungsten ions considered here. For W^{29+} to W^{37+} ions, Jonauskas *et al* (2010) used the FAC code with an extended multiconfiguration basis for computing the *A*-values of 45 M1 lines. Their results, listed in table 3, are in excellent agreement (within a few per cent) with our calculations. In the case of higher ionization stages (W^{39+}–W^{43+}), Fournier (1998) reported oscillator strengths for some M1 lines obtained using the fully relativistic parametric potential code RELAC of Klapisch and coworkers (Aymar *et al* 1970, Klapisch 1971, Klapisch *et al* 1977). The transition probabilities deduced from these *gf*-values are also listed in table 3. Here again, very good agreement (within 5%) is observed except the W^{41+} $4p^3[1]_{3/2}$–$4p^3[3]_{5/2}$ line for which the relative difference is reaching 18%.

At the same time while performing this work, relativistic calculations for M1-type transitions in the $4d^k$ configurations of W^{29+}–W^{37+} ions were also carried out by Jonauskas *et al* (2012) who used the MCDF method implemented in the GRASP2K code (Fischer *et al* 2006, Jönsson *et al* 2007). In the latter study, large discrepancies were obtained for radiative probabilities in comparison with previous FAC data of Jonauskas *et al* (2010), the differences reaching even up to a factor of 3 for some lines. Such discrepancies were not observed when comparing our MCDF data with FAC results. In order to have additional data, we decided to carry out calculations with an independent approach, i.e. the HFR method of Cowan (1981). This method was used in an *ab initio* way with the same sets of configurations as those used in our MCDF calculations and listed in table 1 and it was verified that HFR wavelengths were in very good agreement with MCDF ones. The transition probabilities obtained with the different approaches are compared in table 4 for all observed M1 lines in W^{29+}–W^{37+} ions. As can be seen from this table, our MCDF and HFR results are in very good agreement (within a few per cent) with each other as well as with the FAC calculations of Jonauskas *et al* (2010). In contrast, the new GRASP2K *A*-values of Jonauskas *et al* (2012) show large discrepancies with all of the other three approaches in many cases. In their paper, the latter authors claimed that these discrepancies were essentially due to the larger multiconfiguration basis used in their

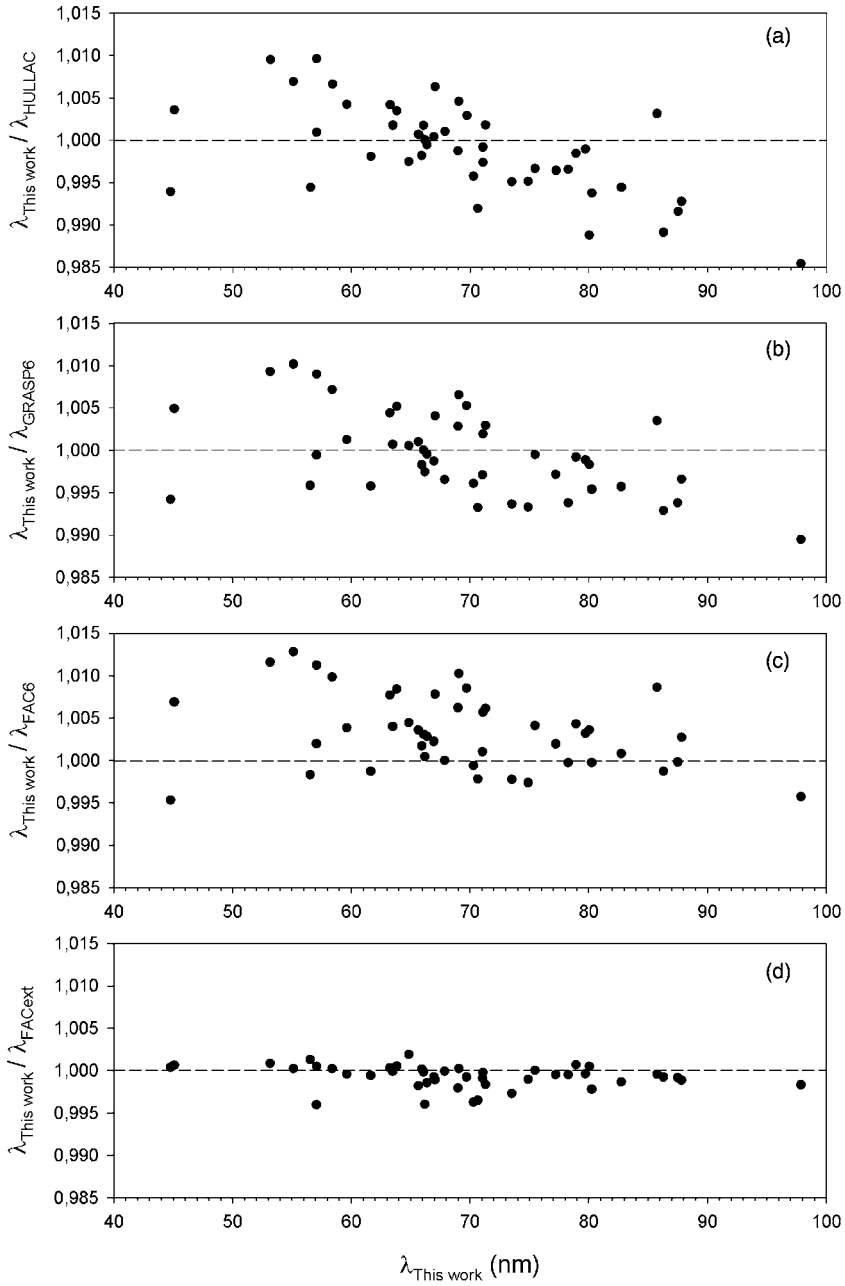

Figure 2. Comparison between wavelengths computed in the present work ($\lambda_{\text{This work}}$) and other theoretical values previously obtained by Radtke *et al* (2007) using the HULLAC code (a) and by Jonauskas *et al* (2010) using the GRASP and FAC packages within six configurations (GRASP6 (b), FAC6 (c)) and the extended basis (FACext (d)).

physical models. To verify this, we performed further HFR calculations using an extended set of configurations in two particular ions, i.e. W^{29+} and W^{37+} for which the GRASP2K *A*-values of Jonauskas *et al* (2012) are respectively a factor of 1.5 smaller and 1.5 larger than our values (obtained with both MCDF and HFR methods) and FAC values published by Jonauskas *et al* (2010). More precisely, for these two ions, the lists of interacting configurations given in table 1 were completed by additional configurations chosen among those having the largest configuration interaction strengths with $4d^k$ as estimated by Jonauskas *et al* (2010). These additional configurations were $4s^24p^44d^k4f^2$, $4s^24p^54d^k5p$, $4s4p^54d^{k+1}4f$, $4s^24p^54d^{k-1}4f5g$, $4s^24p^54d^{k-1}5p5d$, $4s4p^64d^{k-1}4f^2$, $4s^24p^64d^{k-2}5d^2$, $4s4p^64d^k5s$, $4s^24p^64d^{k-1}6d$, $4s^24p^54d^{k-1}4f6g$, $4s^24p^54d^{k-1}4f7g$, $4s^24p^64d^{k-2}5d6d$, $4s^24p^54d^{k-1}4f5d$, $3d^94s^24p^64d^{k-1}4f^2$, $3d^94s^24p^54d^{k+1}4f$, $3d^94s^24p^64d^{k-1}4f5f$, $3d^84s^24p^64d^k4f^2$ and $3d^84s^24p^64d^{k+2}$. It was found that the effect of these configurations on the transition rates was negligible, the variation of *A*-values being smaller than 0.1% for M1 lines within the $4d^9$ (W^{29+}) and 4d (W^{37+}) configurations. This does not seem to confirm that the discrepancies between the GRASP2K data of Jonauskas *et al* (2012) and all the other theoretical calculations are due to missing configurations in the latter models. Following our present work, the origin of these discrepancies remains thus unclear.

Table 4. Comparison of radiative transition probabilities (A in s^{-1}) for experimentally observed M1 lines in W^{29+} through W^{37+} ions. $X(Y)$ stands for $X \times 10^{Y}$.

Ion	Transition	λ_{exp} [a]	A_{MCDF} [b]	A_{HFR} [c]	A_{FAC} [d]	$A_{GRASP2K}$ [e]
W^{29+}	$4d^9[1]_{5/2}$–$4d^9[2]_{3/2}$	75.664	3.74(4)	3.82(4)	3.72(4)	2.48(4)
W^{30+}	$4d^8[1]_4$–$4d^8[7]_4$	57.041	1.71(4)	1.74(4)	1.69(4)	1.69(4)
	$4d^8[4]_3$–$4d^8[8]_2$	67.092	6.52(4)	6.66(4)	6.49(4)	4.65(4)
	$4d^8[2]_2$–$4d^8[6]_1$	68.757	2.54(4)	2.57(4)	2.51(4)	1.51(4)
	$4d^8[2]_2$–$4d^8[5]_2$	79.031	2.83(4)	2.93(4)	2.81(4)	2.82(4)
	$4d^8[1]_4$–$4d^8[4]_3$	79.421	4.71(4)	4.83(4)	4.68(4)	3.66(4)
W^{31+}	$4d^7[1]_{9/2}$–$4d^7[5]_{9/2}$	66.676	3.55(4)	3.64(4)	3.49(4)	3.53(4)
	$4d^7[1]_{9/2}$–$4d^7[4]_{7/2}$	80.488	5.00(4)	5.12(4)	4.97(4)	4.00(4)
W^{32+}	$4d^6[1]_4$–$4d^6[7]_5$	66.108	9.28(3)	9.78(3)	9.20(3)	1.13(4)
	$4d^6[8]_6$–$4d^6[21]_6$	66.819	2.20(4)	2.26(4)	2.18(4)	2.19(4)
	$4d^6[1]_4$–$4d^6[5]_4$	80.303	4.15(4)	4.29(4)	4.07(4)	4.12(4)
W^{33+}	$4d^5[1]_{5/2}$–$4d^5[4]_{3/2}$	69.236	5.63(4)	5.75(4)	5.57(4)	3.71(4)
	$4d^5[1]_{5/2}$–$4d^5[3]_{7/2}$	70.618	2.14(4)	2.27(4)	2.12(4)	2.82(4)
	$4d^5[2]_{5/2}$–$4d^5[11]_{5/2}$	70.822	9.16(4)	9.50(4)	9.03(4)	9.10(4)
W^{34+}	$4d^4[2]_1$–$4d^4[7]_2$	66.240	6.52(4)	6.88(4)	6.45(4)	1.08(5)
	$4d^4[2]_1$–$4d^4[6]_0$	68.060	1.24(5)	1.26(5)	1.23(5)	4.11(4)
	$4d^4[3]_2$–$4d^4[11]_1$	69.695	5.03(4)	5.13(4)	4.97(4)	2.99(4)
	$4d^4[4]_4$–$4d^4[10]_5$	73.664	2.31(4)	2.43(4)	2.29(4)	2.81(4)
	$4d^4[1]_0$–$4d^4[2]_1$	85.563	4.11(4)	4.35(4)	4.08(4)	1.23(5)
	$4d^4[4]_4$–$4d^4[8]_4$	86.451	3.76(4)	3.94(4)	3.70(4)	3.74(4)
W^{35+}	$4d^3[3]_{3/2}$–$4d^3[12]_{5/2}$	56.382	3.64(4)	3.78(4)	3.62(4)	5.45(4)
	$4d^3[7]_{5/2}$–$4d^3[16]_{3/2}$	56.654	3.91(4)	3.23(4)	3.90(4)	2.60(4)
	$4d^3[6]_{9/2}$–$4d^3[13]_{11/2}$	61.534	2.20(4)	2.27(4)	2.19(4)	2.62(4)
	$4d^3[1]_{3/2}$–$4d^3[5]_{1/2}$	62.230	1.39(4)	1.46(4)	1.39(4)	6.94(3)
	$4d^3[3]_{3/2}$–$4d^3[10]_{3/2}$	62.985	6.72(4)	6.89(4)	6.67(4)	6.70(4)
	$4d^3[2]_{5/2}$–$4d^3[8]_{7/2}$	65.920	7.31(4)	7.59(4)	7.27(4)	9.71(4)
	$4d^3[5]_{1/2}$–$4d^3[11]_{1/2}$	66.003	6.71(4)	6.89(4)	6.66(4)	6.69(4)
	$4d^3[1]_{3/2}$–$4d^3[3]_{3/2}$	71.046	3.72(4)	3.77(4)	3.70(4)	3.70(4)
	$4d^3[4]_{7/2}$–$4d^3[9]_{9/2}$	75.664	1.96(4)	2.02(4)	1.95(4)	2.44(4)
	$4d^3[6]_{9/2}$–$4d^3[9]_{9/2}$	77.476	3.18(4)	3.29(4)	3.15(4)	3.17(4)
	$4d^3[1]_{3/2}$–$4d^3[2]_{5/2}$	82.268	4.53(4)	4.77(4)	4.49(4)	6.76(4)
W^{36+}	$4d^2[3]_3$–$4d^2[8]_2$	52.619	1.27(4)	1.28(4)	1.27(4)	9.04(3)
	$4d^2[1]_2$–$4d^2[5]_1$	54.120	3.77(3)	3.86(3)	3.76(3)	2.27(3)
	$4d^2[1]_2$–$4d^2[4]_2$	57.430	2.77(4)	2.84(4)	2.77(4)	2.77(4)
	$4d^2[3]_3$–$4d^2[7]_4$	59.801	5.95(4)	6.13(4)	5.92(4)	7.63(4)
	$4d^2[4]_2$–$4d^2[8]_2$	63.589	4.80(4)	4.92(4)	4.79(4)	4.79(4)
	$4d^2[5]_1$–$4d^2[8]_2$	68.060	2.04(4)	2.13(4)	2.03(4)	3.39(4)
	$4d^2[1]_2$–$4d^2[3]_3$	70.774	5.39(4)	5.59(4)	5.35(4)	7.53(4)
	$4d^2[6]_4$–$4d^2[7]_4$	79.509	1.55(4)	1.60(4)	1.55(4)	1.55(4)
	$4d^2[2]_0$–$4d^2[5]_1$	85.585	2.11(4)	2.26(4)	2.10(4)	6.32(4)
W^{37+}	$4d[1]_{3/2}$–$4d[2]_{5/2}$	64.668	3.93(4)	4.06(4)	3.97(4)	5.87(4)

[a] From Radtke *et al* (2007).
[b] MCDF calculations from this work.
[c] HFR calculations from this work.
[d] FAC calculations from Jonauskas *et al* (2010).
[e] GRASP2K calculations from Jonauskas *et al* (2012).

5. Conclusion

A new set of theoretical wavelengths and transition probabilities has been obtained for forbidden lines within the $4p^k$ and $4d^k$ ground configurations of multicharged tungsten ions. These results are intended to help plasma physicists with line identifications and interpretation of spectra emitted by plasmas produced in fusion reactors. The accuracy of the present data was tested by comparison with some available experimental and theoretical wavelengths and with transition rates previously calculated for a few lines using different computational approaches. Our new wavelengths are in excellent agreement with the EBIT measurements and with the most reliable calculations performed previously. Concerning the radiative transition probabilities, although our MCDF results are in excellent agreement with data obtained using other approaches (HFR, FAC), unexpected large differences remain with the recent GRASP2K results of Jonauskas

et al (2012). However, our detailed analysis does not seem to demonstrate that such differences can be explained by missing configurations in our physical models.

Acknowledgments

The author is Senior Research Associate of the Belgian FRS-FNRS. Financial support from this organization is acknowledged.

References

Aymar M, Crance M and Klapisch M 1970 *J. Physique* **31** C4
Charro E, Curiel Z and Martin I 2002 *Astron. Astrophys.* **387** 1146
Charro E, Lopez-Ferrero S and Martin I 2003 *Astron. Astrophys.* **406** 741
Clementson J, Beiersdorfer P and Gu M F 2010 *Phys. Rev.* A **81** 012505
Cowan R D 1981 *The Theory of Atomic Structure and Spectra* (Berkeley, CA: University of California Press)
Doron R and Feldman U 2001 *Phys. Scr.* **64** 319
Feldman U, Doron R, Klapisch M and Bar-Shalom A 2001 *Phys. Scr.* **63** 284
Feldman U, Indelicato P and Sugar J 1991 *J. Opt. Soc. Am.* B **8** 3
Fischer C F, Gaigalas G and Ralchenko Y 2006 *Comput. Phys. Commun.* **175** 738
Fournier K B 1998 *At. Data Nucl. Data Tables* **68** 1
Fullerton L W and Rinker G A 1976 *Phys. Rev.* A **13** 1283
Grant I P and McKenzie B J 1980 *J. Phys. B: At. Mol. Phys.* **13** 2671
Grant I P, McKenzie B J, Norrington P H, Mayers D F and Pyper N C 1980 *Comput. Phys. Commun.* **21** 207
Hawryluk R J *et al* 2009 *Nucl. Fusion* **49** 065012
Huang K N 1984 *At. Data Nucl. Data Tables* **30** 313
Huang K N 1985 *At. Data Nucl. Data Tables* **32** 503
Huang K N 1986 *At. Data Nucl. Data Tables* **34** 1
Huang K N, Kim Y K, Cheng K T and Desclaux J P 1983 *At. Data Nucl. Data Tables* **28** 355
Jonauskas V, Gaigalas G and Kucas S 2012 *At. Data Nucl. Data Tables* **98** 19
Jonauskas V, Kisielius R, Kyniene A, Kucas S and Norrington P H 2010 *Phys. Rev.* A **81** 012506
Jönsson P, He X, Fischer C F and Grant I P 2007 *Comput. Phys. Commun.* **177** 597
Klapisch M 1971 *Comput. Phys. Commun.* **2** 239
Klapisch M, Schwob J L, Fraenkel B and Oreg J 1977 *J. Opt. Soc. Am.* **67** 148
Kramida A E and Shirai T 2006 *J. Phys. Chem. Ref. Data* **35** 423
Kramida A E and Shirai T 2009 *At. Data Nucl. Data Tables* **95** 305
Matthews G F *et al* 2007 *Phys. Scr.* T **128** 137
McKenzie B J, Grant I P and Norrington P H 1980 *Comput. Phys. Commun.* **21** 233
Mohr P J 1974 *Ann. Phys.* **88** 52
Mohr P J 1975 *Phys. Rev. Lett.* **34** 1050
Neu R, Fournier K B, Bolshukhin D and Dux R 2001 *Phys. Scr.* T **92** 307
Neu R, Fournier K B, Schlögl D and Rice J 1997 *J. Phys. B: At. Mol. Opt. Phys.* **30** 5057
Norrington P H 2009 http://www.am.qub.ac.uk/DARC/
Pitts R A *et al* 2009 *Phys. Scr.* T **138** 014001
Porto J V, Kink I and Gillaspy J D 2000 *Phys. Rev.* A **61** 054501
Pütterich T, Neu R, Biedermann C, Radtke R and ASDEX Upgrade Team 2005 *J. Phys. B: At. Mol. Opt. Phys.* **38** 2071
Quinet P 2011 *J. Phys. B: At. Mol. Opt. Phys.* **44** 195007
Quinet P, Vinogradoff V, Palmeri P and Biémont E 2010 *J. Phys. B: At. Mol. Opt. Phys.* **43** 144003
Radtke R, Biedermann C, Fussmann G, Schwob J L, Mandelbaum P and Doron R 2007 *Atomic and Plasma-Material Interaction Data for Fusion* vol 13 (Vienna: IAEA)
Ralchenko Y, Draganic I N, Osin D, Gillaspy J D and Reader J 2011a *Phys. Rev.* A **83** 032517
Ralchenko Y, Draganic I N, Tan J N, Gillaspy J D, Pomeroy J M, Reader J, Feldman U and Holland G E 2008 *J. Phys. B: At. Mol. Opt. Phys.* **41** 021003
Ralchenko Y, Kramida A E, Reader J and NIST ASD Team 2011b *NIST Atomic Spectra Database v.4.1.0*
Ralchenko Y, Reader J, Pomeroy J M, Tan J N and Gillaspy J D 2007 *J. Phys. B: At. Mol. Opt. Phys.* **40** 3861
Ralchenko Y, Tan J N, Gillaspy J D, Pomeroy J M and Silver E 2006 *Phys. Rev.* A **74** 042514
Safronova U I and Safronova A S 2010 *J. Phys. B: At. Mol. Opt. Phys.* **43** 074026
Saloman E B and Kim Y K 1989 *At. Data Nucl. Data Tables* **41** 339
Tragin N, Geindre J-P, Monier P, Gauthier J-C, Chenais-Popovics C, Wyart J-C and Bauche-Arnoult C 1988 *Phys. Scr.* **37** 72
Utter S B, Beiersdorfer P and Brown G V 2000 *Phys. Rev.* A **61** 030503
Utter S B, Beiersdorfer P and Trabert E 2002 *Can. J. Phys.* **80** 1503